MASSACHUSETTS INSTITUTE OF TECHNOLOGY
LINCOLN LABORATORY

DATA MODULATION FOR A DIRECT SEQUENCE PSEUDONOISE SPREAD SPECTRUM COMMUNICATION SYSTEM

A.L. KACHELMYER
Group 52

PROJECT REPORT IFF-7

29 SEPTEMBER 1981

LEXINGTON MASSACHUSETTS

CONTENTS

LIST OF FIGURES

LIST OF FIGURES, cont'd

LIST OF FIGURES, cont'd

1.0 INTRODUCTION

M-ary differential phase shift keying (MDPSK) and M-ary incoherent orthogonal keying (MOK) are to be evaluted as possible data modulation options for a direct PN spread spectrum IFF system. MOK and MDPSK are two basic modulation techniques which do not require a phase coherent carrier reference for demodulation and which are compatible with an acousto-electric convolver based receiver.

The transmitted PN spread spectrum waveform can be represented as

$$s(t) = A \, \mathrm{Re} \{ e^{j(\omega_o t + \Phi(t))} \} \qquad (1.1)$$

where

$$\Phi(t) = \phi^i(t) \quad , \quad (i-1)T < t < iT \qquad (1.2)$$

and

A is the amplitude of the constant envelope,

ω_o is the angular carrier frequency,

$\phi^i(t)$ is one of M possible PN phase waveforms over the i^{th} data symbol time,

T is the data symbol duration.

In the case of MOK, $\phi^i(t)$ is one of M orthogonal PN phase waveforms. In general, the M-ary signalling set may consist of M distinct PN sequences. If BPSK spreading is used, then the MOK phase waveform may be expressed as

$$\phi^i(t) = \phi_c(t) + \theta_d(t) \qquad (1.3)$$

where $\phi_c(t)$ is a single PN chipping sequence and $\theta_d(t)$ is one of M phase waveforms which are orthogonal over the data symbol period T. For instance, $\theta_d(t)$ may be one of M distinct Walsh functions which takes on the values 0 or π radians. This is equivalent to multiplying the BPSK waveform by Walsh functions which take on +1 or -1 values.

In the case of MDPSK, the phase waveform may be expressed as

$$\phi^i(t) = \phi_c(t) + \frac{2\pi}{M} (K - 1) \quad , \quad 1 \leq K \leq M \qquad (1.4)$$

where the data message consists of the K^{th} phase value.

The performance criteria used to evaluate a particular option include waveform sensitivity to relative motion (doppler shift) between the interrogator and transponder, required signal-to-noise ratio per symbol E_s/N_o or per bit E_b/N_o at the output of the matched filters for a fixed symbol error probability, message length required (with fixed symbol durations), and implementation complexity (especially in terms of acousto-electric convolver implementations).

2.0 CALCULATION OF THE PROBABILITY OF A DATA SYMBOL ERROR P_{SE} FOR MDPSK AND MOK

The proposed IFF system will employ PN spectrum spreading with N chips of duration τ_c for every data symbol. The performance of a particular data modulation technique is measured in terms of the probability of the signal-to-noise ratio E_s/N_o at the output of the receiver matched filters. E_s is the total signal energy in N chips (per data symbol) and the double-sided noise spectral density is $N_o/2$ watts/Hz.

By considering E_s/N_o, we can compare the modulation techniques while fixing the total energy available in a T second data symbol interval ($T=N\tau_c$). Notice that in the differentially coherent system we are using the energy over a 2T second interval ($2E_s$) at each decision time (noise is correlated from sample to sample). It is assumed that the receiver is time synchronized so that the total signal energy is available at the sample times.

In the differentially coherent system, the phase of the local oscillator at the receiver is assumed to be constant but independent of the phase of the transmitted signal. In the coherent orthogonal system, the demodulation reference signals need only maintain constant phase over each T second interval.

2.1 M-Ary Differential Phase Shift Keying (MDPSK)

Ignoring the modulation and demodulation of the PN chipping sequence,

the transmitted MDPSK signal set can be represented as

$$s^i(t) = \sqrt{\frac{2E_s}{T}} \sin(\omega_o t + \theta_d{}^i(t)), \quad (i-1)T \leq t \leq iT \tag{2.1}$$

where $\theta_d{}^i(t)$ is the message phase over the i^{th} time interval and where

$$\theta_k = \frac{2\pi}{M}(k-1) \quad \text{for } k = 1, 2, \ldots, M \tag{2.2}$$

represents the M possible message phases. In block diagram form the receiver can be implemented as shown in Fig. 2.1.

The probability of a symbol error is the probability that the measured phase difference differs from the actual phase difference by more than π/M; that is

$$P_{SE}(\text{MDPSK}) = P_r\left[|\psi| = \left|\left(\eta^i - \eta^{i-1}\right) - \left(\theta^i - \theta^{i-1}\right)\right| > \pi/M\right]$$

$$= 1 - \int_{-\pi/M}^{\pi/M} p_\psi(x)\,dx = 2\int_{\pi/M}^{\pi} p_\psi(x)\,dx. \tag{2.3}$$

Thus, we need the probability density function of the random variable ψ.

The received signal during the i^{th} time interval is

$$r(t) = s^i(t) + n(t) \qquad (i-1)T \leq t \leq iT. \tag{2.4}$$

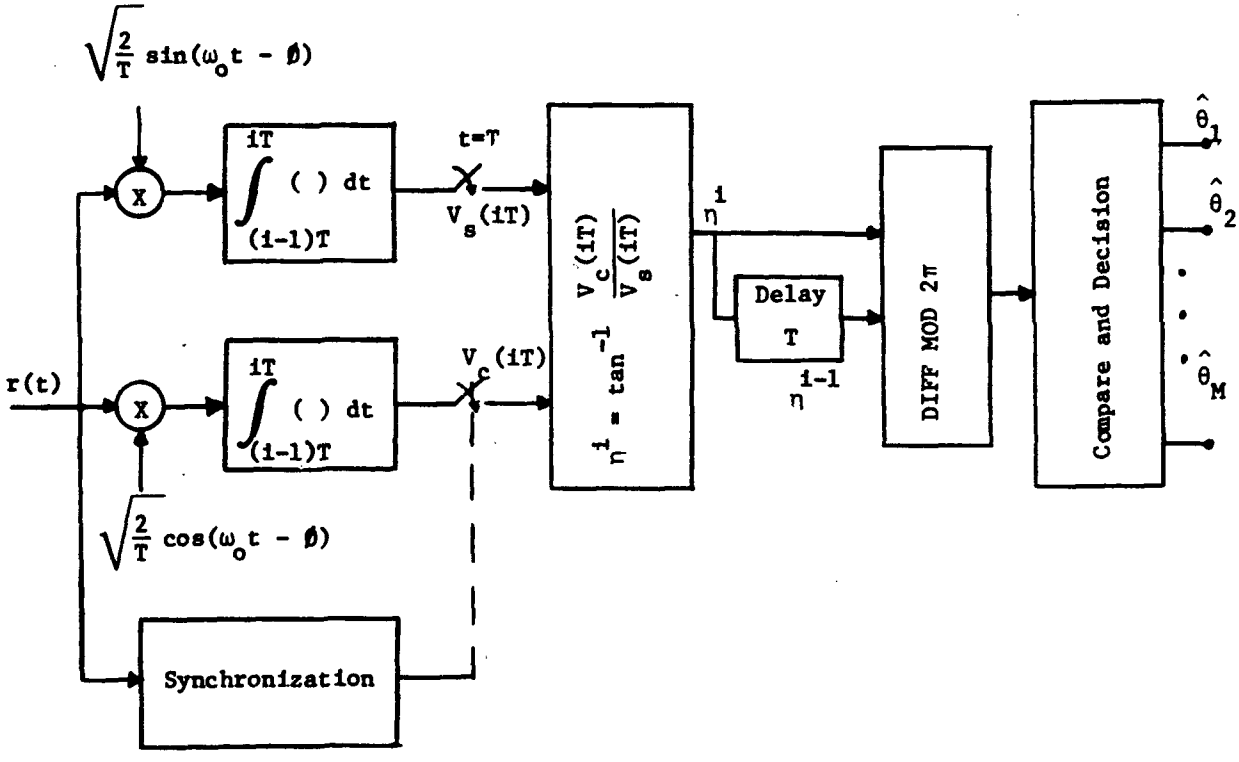

Fig. 2.1. General M-ary DPSK receiver.

The integrator outputs become

$$V_s(iT) = \int_{(i-1)T}^{iT} \sqrt{2/T} \sin(\omega_o t - \phi)\, r(t)\, dt$$

$$= \sqrt{E_s} \cos(\phi + \theta^i) + n_s(iT) \tag{2.5}$$

and

$$V_c(iT) = \sqrt{E_s} \sin(\phi + \theta^i) + n_c(iT) \tag{2.6}$$

where

$$n_s(iT) = \int_{(i-1)T}^{iT} \sqrt{2/T} \sin(\omega_o t - \phi)\, n(t)\, dt, \tag{2.7}$$

$$n_c(iT) = \int_{(i-1)T}^{iT} \sqrt{2/T} \cos(\omega_o t - \phi)\, n(t)\, dt. \tag{2.8}$$

Notice that the energy per data symbol of duration T is E_s. Assuming the noise samples n_s and n_c are normally distributed with variances $N_o/2$, the pdfs of the integrator output samples are

$$p_{V_s(iT)}(x) = \frac{1}{\sqrt{\pi N_o}} e^{-(x - \sqrt{E_s}\cos(\theta^i + \phi))^2/N_o}, \tag{2.9}$$

$$p_{V_c(iT)}(x) = \frac{1}{\sqrt{\pi N_o}} e^{-(y - \sqrt{E_s}\sin(\theta^i + \phi))^2/N_o}. \tag{2.10}$$

The next step is to find the pdf of the random variable η^i, where

$$\eta^i = \tan^{-1} \frac{V_c(iT)}{V_s(iT)} \quad . \tag{2.11}$$

Since V_c and V_s are independent, the cumulative probability distribution of η^i becomes (dropping the function of iT notation for convience)

$$P[\eta^i \leq n] = P\left[\tan^{-1} \frac{V_c}{V_s} \leq n\right]$$

$$= P\left[\frac{V_c}{V_s} \leq \tan n\right]$$

$$= \int_{-\infty}^{0} \int_{V_s \tan n}^{\infty} p_{Vs}(v_s)\, p_{Vc}(v_c)\, dv_c dv_s + \int_{0}^{\infty} \int_{-\infty}^{v_s \tan n} p_{Vs}(v_s)\, p_{Vc}(v_c)\, dv_c dv_s \quad . \tag{2.12}$$

Hence, the pdf of η^i becomes

$$p_{\eta^i}(n) = \frac{d}{dn} P[\eta^i \leq n] = 2 \int_0^{\infty} v_s \sec^2 n\, p_{Vs}(v_s)\, p_{Vc}(v_s \tan n)\, dv_s \quad -\pi/2 \leq n \leq \pi/2$$

$$= \begin{cases} \int_0^{\infty} \frac{r}{\pi} e^{-\left[r^2 - 2r\sqrt{\frac{E_s}{N_o}} \cos(n - \theta^i - \phi) + E_s/N_o\right]} dr & 0 \leq n \leq 2\pi \\ 0 & \text{otherwise} \end{cases} \tag{2.13}$$

Letting $\theta = \theta^i - \theta^{i-1}$ it follows that $\Psi = \eta^i - \eta^{i-1} - \theta$ and since η^i and η^{i-1} are statistically independent, the pdf of Ψ becomes

$$p_{\psi}(x) = \int_{-\pi}^{\pi} p_{\eta i}\,(x + y + \theta)\; p_{\eta i-1}\,(y)\; dy$$

$$= \int_{-\pi}^{\pi} \left\{ \int_{o}^{\infty} \frac{r}{\pi}\, e^{-(r^2 - 2r\sqrt{\frac{E_s}{N_o}}\,\cos\,(x + y - \theta^{i-1} - \phi) + \frac{E_s}{N_o})}\, dr \cdot \int_{o}^{\infty} \frac{u}{\pi} \right.$$

$$\left. \cdot e^{-\,(u^2 - 2u\sqrt{\frac{E_s}{N_o}}\,\cos\,(y - \theta^{i-1} - \phi) + \frac{E_s}{N_o})}\, du \right\} dy \quad . \qquad (2.14)$$

Using the method of characteristic functions, Fleck and Trabka [2] have shown that (2.14) can be reduced to

$$p_{\psi}(x) = \frac{1}{2\pi} \int_{o}^{\pi/2} \left[1 + \frac{E_s}{N_o}\,(1 + \cos x\, \sin\alpha) \right] e^{-\frac{E_s}{N_o}\,(1 - \cos x\, \sin\alpha)}$$

$$\cdot \sin\alpha\, d\alpha \qquad (2.15)$$

Using the theory of Bessel functions (2.15) can be integrated to yield

$$p_{\psi}(x) = p_{\psi}\,(\pi/2) + \tfrac{1}{4}\,\frac{E_s}{N_o} \cdot e^{-\frac{E_s}{N_o}} \left\{ I_1\left(\frac{E_s}{N_o}\cos x\right) + L_1\left(\frac{Es}{N_o}\cos x\right) \right.$$

$$\left. + \cos x \left[I_o\left(\frac{E_s}{N_o}\cos x\right) + L_o\left(\frac{E_s}{N_o}\sin x\right) \right] \right\} \qquad (2.16)$$

where $I_n(x)$ and $L_n(x)$ are the modified Bessel function and Sturve function, respectively. The probability density function of the phase difference $p_\psi(x)$ is plotted in Fig. 2.2 for several values of E_s/J_o.

The exact expression for the probability of a symbol error is thus given by (2.3) with $p_\psi(x)$ specified by (2.15) or (2.16).

Several attempts have been made to approximate (2.3) for reasonable large signal-to-noise ratios. Fleck and Trabka [2] have found

$$P_{SE}\,(\text{MDPSK}) \cong \text{erfc}[u] + \frac{ue^{-u^2}}{4\sqrt{\pi}\left(1/8 + E_s/N_o\right)} \quad ; \; u = \sqrt{2E_s/N_o}\sin\frac{\pi}{2M} \; . \tag{2.17}$$

Arthurs and Dym [3] show that

$$P_{SE}\,(\text{MDPSK}) \cong \text{erfc}\left[\sqrt{E_s/N_o}\sin\frac{\pi}{\sqrt{2}M} \; .\right] \tag{2.18}$$

Bussgang and Leiter [4] derived an upper bound which approximates closely for $E_s/N_o > 5$ dB. It is

$$P_{SE}\,(\text{MDPSK}) \cong \text{erfc}\left[\frac{E_s/N_o}{\sqrt{1 + 2E_s/N_o}}\sin\pi/M \right] \; . \tag{2.19}$$

The MDPSK probability of a symbol error versus the symbol signal-to-noise ratio E_s/N_o (at the outputs of the integration filters of Fig. 2.1) is plotted in Fig. 2.5 for M = 2, 4, 8 and 16.

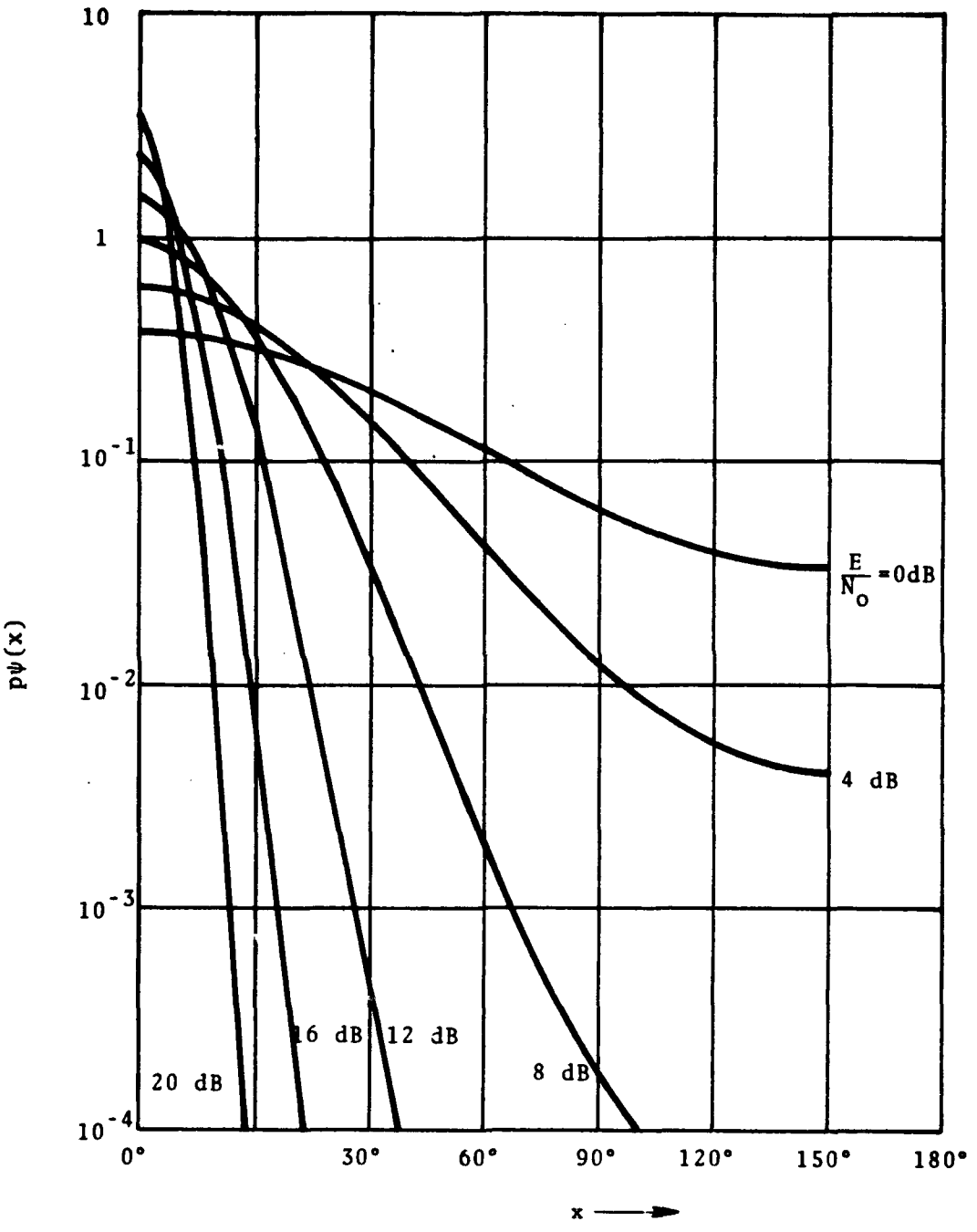

Fig. 2.2 Probability density of phase difference.

2.2 M-ary Incoherent Orthogonal Keying (MOK)

The message set for the MOK technique is defined in terms of the M possible orthogonal phase waveforms $\theta_k(t)$, where k = 1, 2, ..., M. The data phase waveform can be arbitrary, but must have the orthogonal property that

$$\int_0^T \theta_i(t)\, \theta_j(t)\, dt = 0 \qquad \text{for } i \neq j \tag{2.20}$$

where T is the symbol duration.

If we desire to send the k^{th} message during the i^{th} time interval, then the data phase waveform becomes

$$\theta_d{}^i(t) = \theta_k(t) \qquad (i-1)T < t < iT\ . \tag{2.21}$$

The M orthogonal phase waveforms can be formed by bi-phase keying the transmitted signal over subsections of the T second symbol interval. For example, with a 4-ary system the phase waveforms could be constructed as shown in Fig. 2.3.

The general block diagram form of the MOK receiver is shown in Fig. 2.4.

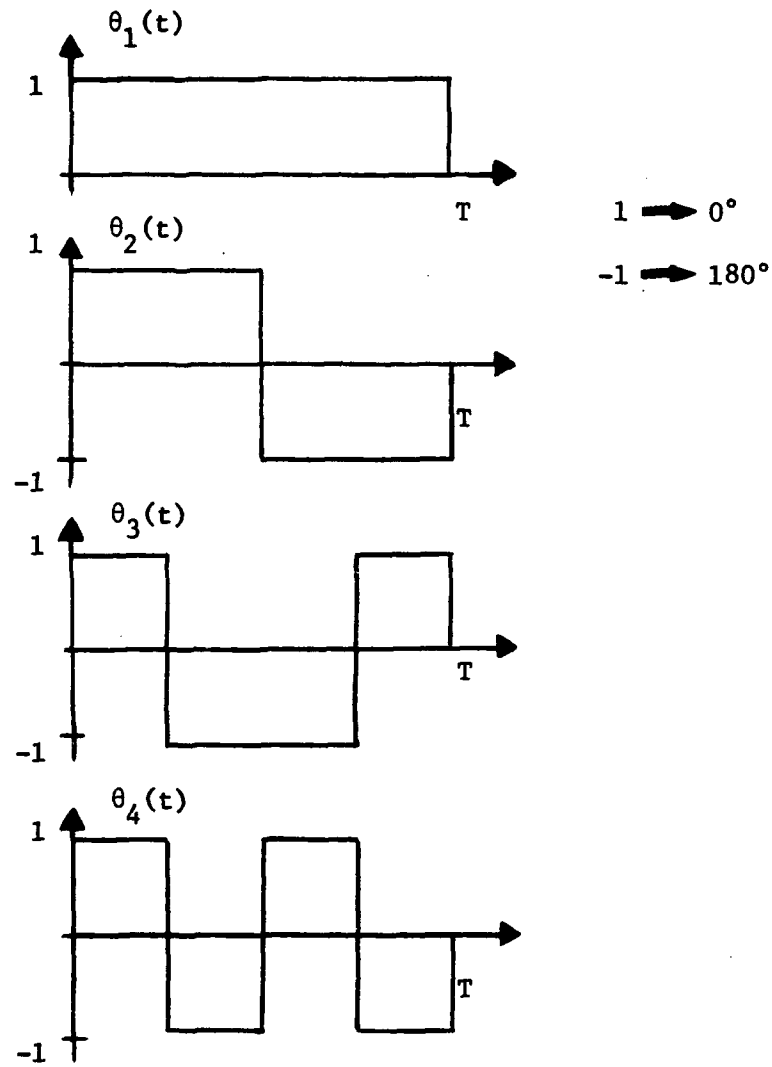

Fig. 2.3. Orthogonal message waveforms.

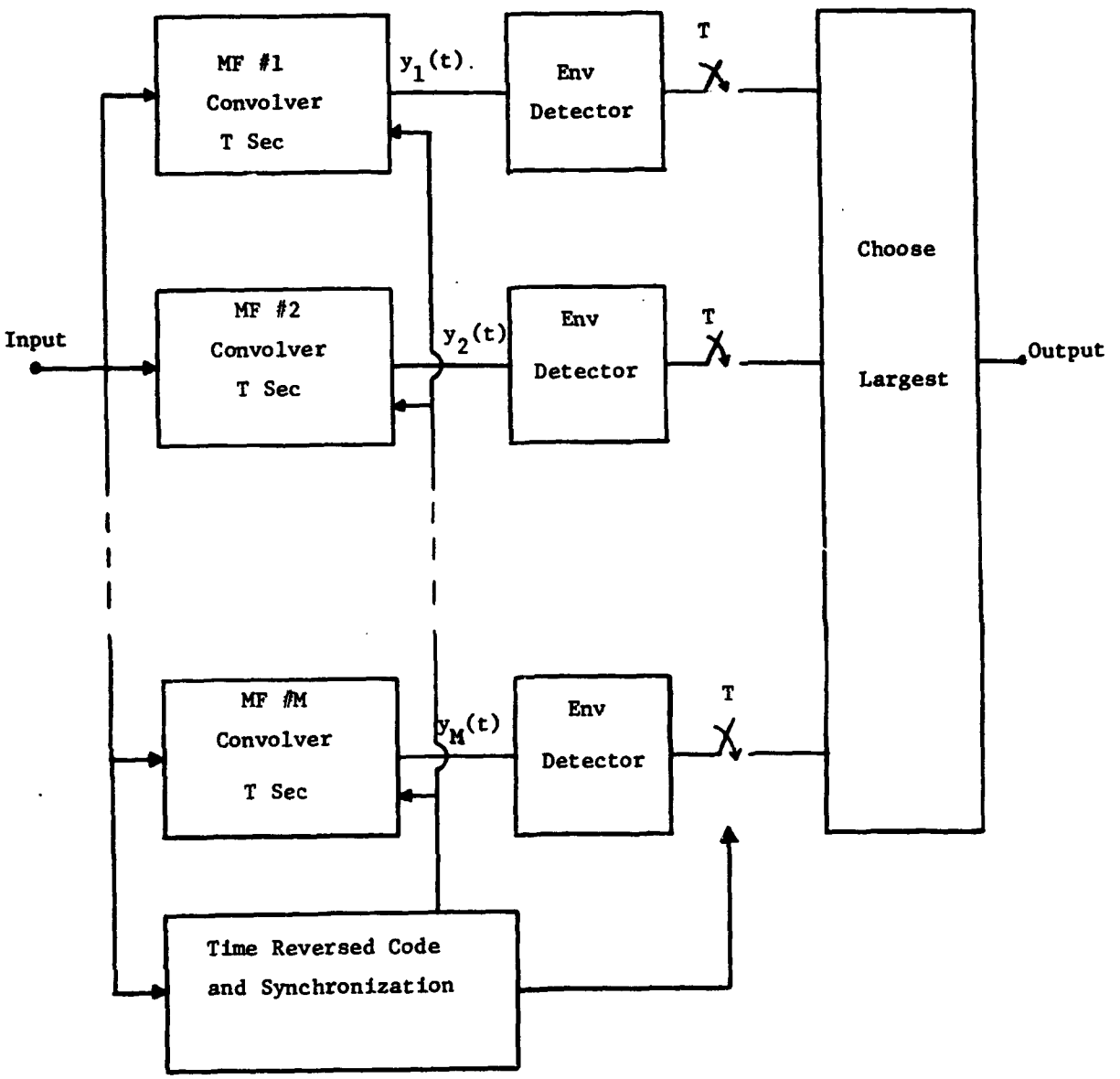

Fig. 2.4. M-ary matched filter receiver.

Let ε_i; i = 1, 2, ... M represent the M envelope samples at time t = T. Given that the first message was sent, the probability of a correct decision is

$$P_C(\text{MOK}) = P\left[\varepsilon_1 > \varepsilon_2, \varepsilon_1 > \varepsilon_3, \ldots, \varepsilon_1 > \varepsilon_M\right] . \tag{2.22}$$

Assuming the samples are independent random variables, the joint density is given by

$$p_{\varepsilon_1, \varepsilon_2 \ldots \varepsilon_M}(\varepsilon_1, \varepsilon_2, .., \varepsilon_M) = p_{\varepsilon_1}(\varepsilon_1)\, p_{\varepsilon_2}(\varepsilon_2) \,..\, p_{\varepsilon_M}(\varepsilon_M) \tag{2.23}$$

where

$$p_{\varepsilon_1}(x) = \frac{x}{N} e^{-(x^2 + E_s)/2N} I_o\left(x\sqrt{\frac{E_s}{N}}\right) \qquad 0 \le x < \infty \tag{2.24}$$

(Rician)

and

$$p_{\varepsilon_i}(y) = y/N\, e^{-y^2/2N} \quad ; \quad i = 2, 3, \ldots, M \qquad 0 \le y < \infty . \tag{2.25}$$

(Rayleigh)

Notice that $N = N_o/2$ is the noise variance. The probability of a message symbol error is

$$P_{SE}(\text{MOK}) = 1 - P_C(\text{MOK})$$

$$= 1 - \int_o^\infty p_{\varepsilon_1}(x) \left[\int_o^x p_{\varepsilon_2}(y)\, dy\right]^{M-1} dx \tag{2.26}$$

But,

$$\int_0^x p_{\epsilon_2}(y)\,dy = \int_0^x \frac{y}{N} e^{-y^2/2N}\,dy = 1 - e^{-x^2/2N} \quad . \tag{2.27}$$

Hence, (2.26) becomes

$$P_{SE}(MOK) = 1 - \int_0^\infty \frac{x}{N} e^{-(x^2 + E_s/2N)} I_o\left(x\sqrt{\frac{E_s}{N}}\right)\left[1 - e^{-x^2/2N}\right]^{M-1} dx. \tag{2.28}$$

As in Arthurs and Dym [3], the binominal expansion can be used to write

$$\left[1 - e^{-x^2/2N}\right]^{M-1} = \sum_{k=0}^{M-1} \binom{M-1}{k} (-1)^k e^{-\frac{x^2}{2N}k} \quad . \tag{2.29}$$

Thus, (2.28) becomes

$$P_{SE}(MOK) = 1 - e^{-E_s/2N} \sum_{k=0}^{M-1} \binom{M-1}{k} (-1)^k \int_0^\infty re^{-\frac{r}{2}(1+k)} I_o\left(r\sqrt{\frac{E_s}{N}}\right)dr. \tag{2.30}$$

The integral in (2.30) is

$$\int_0^\infty re^{-\frac{r^2}{2}(k+1)} I_o\left(r\sqrt{\frac{E_s}{N}}\right)dr = \frac{1}{k+1} e^{\frac{E_s}{2N}(k+1)} \quad . \tag{2.31}$$

Using this result and substituting $N = N_o/2$, the average probability of a symbol error becomes

$$P_{SE}(MOK) = 1 - e^{-E_s/N_o} \sum_{k=0}^{M-1} \binom{M-1}{k} (-1)^k \frac{e^{E_s/N_o (k+1)}}{(k+1)}$$

$$= -e^{E_s/N_o} \sum_{k=1}^{M-1} \binom{M-1}{k} (-1)^k \frac{e^{E_s/N_o (k+1)}}{(k+1)} \quad . \tag{2.32}$$

Noting that

$$\binom{M-1}{k} \frac{1}{k+1} = \binom{M}{k+1} \frac{1}{M} \tag{2.33}$$

and letting $q = k + 1$, the final form is

$$P_{SE}(MOK) = \frac{e^{-E_s/N_o}}{M} \sum_{q=2}^{M} \binom{M}{q} (-1)^q e^{E_s/N_o} \tag{2.34}$$

The MOK probability of a symbol error versus the symbol signal-to-noise ratio E_s/N_o at the matched filter outputs is plotted in Fig. 2.5 for M = 2, 4, 8 and 16.

As expected, DSPK is 3 dB better than binary orthogonal simply because the convolution is performed over a 2T second interval with DPSK.

The interesting result is that in the M-ary orthogonal case higher order symbol alphabets can be used without significant penalty in terms of the required signal-to-noise ratio. Other practical considerations including ease of implementation will have to be investigated in order to determine the optimum value of M.

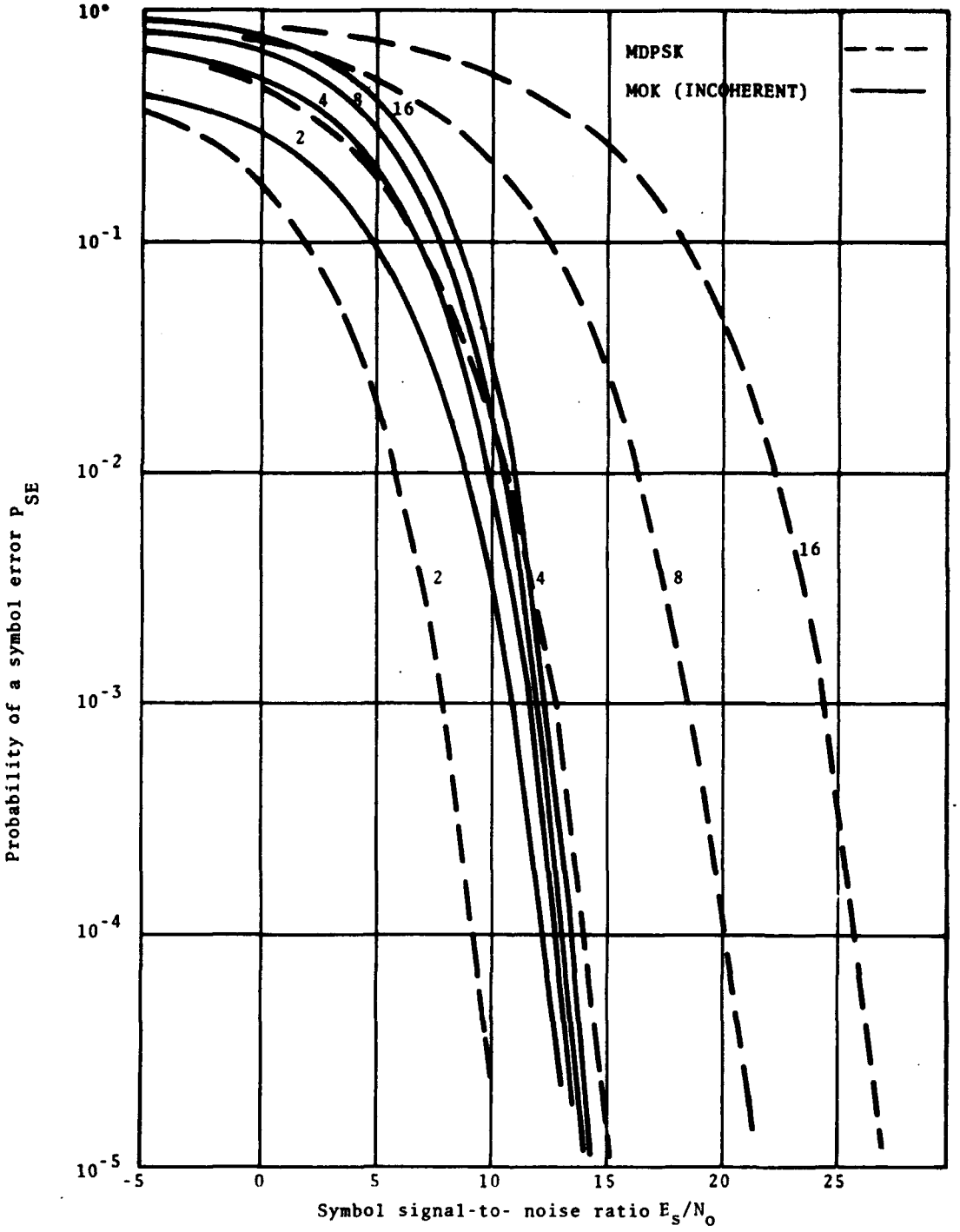

Fig. 2.5. Performance comparison of MDPSK and MOK for M = 2, 4, 8 and 16 (E_s is the energy per symbol).

In the MDPSK system it is unlikely that one would ever consider going beyond the 4-ary or QDPSK system simply because of the signal-to-noise ratio penalties.

2.3 MDPSK with Doppler Shift

The probability of a symbol error for either the MDPSK technique or the MOK technique is a function of the relative motion (doppler shift) between the interrogator and the transponder.

Suppose the received MDPSK signal is doppler shifted with frequency offset ω_d relative to the local reference signal. Then the received signal over the i^{th} time interval is

$$r(t) = \sqrt{\frac{2E_s}{T}} \sin [(\omega_o + \omega_d)t + \theta^i] + n(t) \quad (i-1)T \leq t \leq iT \qquad (2.35)$$

where the message phase θ^i over the i^{th} time interval is one of the M values defined by (2.2).

The outputs of the interogators in Fig. 2.1 become

$$V_s(iT) = \sqrt{2/T} \int_{(i-1)T}^{iT} r(t) \sin (\omega_o t - \phi)dt$$

$$= \sqrt{E_s}\,\mathrm{sinc}\, \omega_d T/2 \cos [(i - 1/2)\, \omega_d T + \theta^i + \phi] + n_s(iT) \qquad (2.36)$$

and

$$V_c(iT) = \sqrt{E_s}\,\mathrm{sinc}\ \omega_d T/2 \sin\left[(1 - 1/2)\omega_d T + \theta^i + \phi\right] + n_c(iT) \ . \quad (2.37)$$

Define the effective energy E' as

$$E' = E_s \mathrm{sinc}^2\ \omega_d T/2 \ . \quad (2.38)$$

Again, assuming the noise samples are normally distributed, the pdf's of the integrator output samples are

$$p_{V_s(iT)}(x) = \frac{1}{\sqrt{\pi N_o}}\, e^{-(x - \sqrt{E'}\cos[(i-1/2)\omega_d T + \theta^i + \phi])^2/N_o} \quad (2.39)$$

$$p_{V_c(iT)}(x) = \frac{1}{\sqrt{\pi N_o}}\, e^{-(x - \sqrt{E'}\sin[(i-1/2)\omega_d T + \theta^i + \phi])^2/N_o} \quad (2.40)$$

The corresponding probability density function of η^i is

$$P_{\eta^i}(n) = \begin{cases} \int_o^\infty e^{-[r^2 - 2r\sqrt{E'/N_o}\cos(n-(i-1/2)\omega_d T - \theta^i - \phi) + E'/N_o]}\, dr & -\pi \le n \le \pi \\ 0 & \text{otherwise} \end{cases} \quad (2.41)$$

Notice that there is a doppler phase shift of $\omega_d T$ between consecutive integrator output samples. Define the shifted phase differences between samples as

$$\psi' = \psi_d - \omega_d T \tag{2.42}$$

where the phase difference in the doppler case is $\psi_d = \eta^i - \eta^{i-1} - \theta^i + \theta^{i-1}$. Using (2.41), it can be shown that the probability density function of ψ' is

$$p_{\psi'}(x) = p_{\psi}(x) \tag{2.43}$$

where $p_{\psi}(x)$ is zero doppler probability density function given by (2.14) with E_s replaced everywhere by E'. The probability of a symbol error can be written from (2.3) as

$$\begin{aligned} P_{SE}\ (\text{MDPSK}) &= 2 \int_{\pi/M}^{\pi} p_{\psi d}(x)dx \\ &= 2 \int_{\pi/M}^{\pi} p_{\psi'}(x-\omega_d T)dx \\ &= 2 \int_{\pi/M}^{\pi} \int_{-\omega_d T}^{-\omega_d T} p_{\psi}(x)dx \end{aligned} \tag{2.44}$$

where $p_\psi(x)$ is given by (2.16) with E_S replaced everywhere by E'.

The probability of a symbol error P_{SE} (MDPSK) for the binary and 4-ary cases are plotted in Fig. 2.6 versus doppler shift $\omega_d T$ for fixed signal-to-noise ratios of 5, 10, and 15 dB.

On a signal-to-noise ratio per bit basis, the solid curves in Fig. 2.6 for QDPSK correspond to 2, 7 and 12 dB. It becomes clear that QDPSK is more sensitive to doppler than BDPSK.

2.4 MOK with Doppler Shift

Due to relative motion between the interrogator and transponder, assume the received MOK signal is doppler shifted (with respect to the carrier frequency) with angular frequency offset ω_d. If the transmitted symbol is matched to the first filter, then with no noise the amplitude of the envelope sample at time t=T due to the first filter output is

$$\sqrt{E_1} = \sqrt{E_s}\ |\text{sinc}\ \omega_d T/2| \tag{2.45}$$

where E_s is the symbol energy and T is the symbol duration. In addition to reducing the amplitude of the true matched filter, the doppler shift also causes a response to the received symbol in the other M-1 not true matched filters.

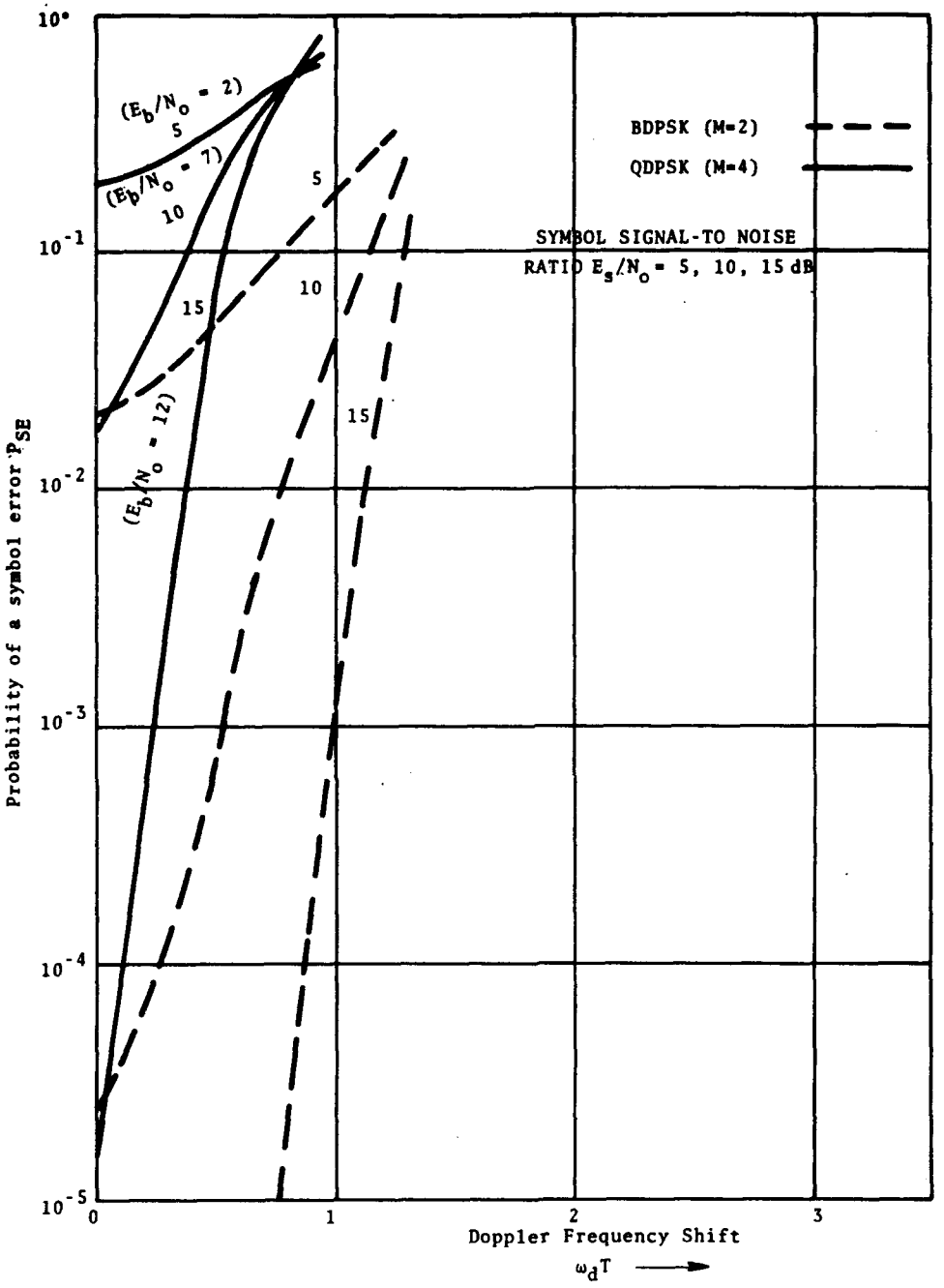

Fig. 2.6. Probability of a symbol error versus doppler shift for BDPSK and QDPSK.

The envelope samples of the outputs of the M matched filters are random variables with probability density functions (Rician) given by

$$f_{\varepsilon_i}(x) = \frac{2x}{N_o} e^{-(x^2 + E_i)/N_o} I_o\left(2x\frac{\sqrt{E_i}}{N_o}\right) \quad 0<x<\infty \quad i=1,2,\ldots M \tag{2.46}$$

where $\sqrt{E_i}$ is the amplitude of the envelope samples due to the doppler shifted message signal only.

Assuming the message matched to filter 1 is sent, the average symbol error probability with doppler frequency offset ω_d is

$$\begin{aligned} P_{SE}(MOK) &= 1 - P_c(MOK) \\ &= 1 - \int_o^\infty f_{\varepsilon_1}(x) \prod_{i=2}^{M} \left\{\int_o^x f_{\varepsilon_i}(y)\, dy\right\} dx . \end{aligned} \tag{2.47}$$

But, we know that

$$\int_o^x f_{\varepsilon_1}(y)\, dy = 1 - Q\left(\sqrt{\frac{2E_1}{N_o}}, \sqrt{\frac{2}{N_o}}\, x\right) \tag{2.48}$$

where the Q function is defined as

$$\begin{aligned} Q(a,b) &= \int_b^\infty x e^{-(a^2 + x^2)/2} I_o(ax)\, dx \\ &= 1 - e^{-(a^2 + b^2)/2} \sum_{m=1}^{\infty} \left(\frac{b}{a}\right)^m I_m(ab) . \end{aligned} \tag{2.49}$$

Thus,

$$P_{SE}(MOK) = 1 - \frac{2}{N_o} e^{-E_1/N_o} \int_o^\infty x e^{-x^2/N_o} I_o\left(\frac{2\sqrt{E_1}x}{N_o}\right) \prod_{i=2}^{M}$$

$$\left(1 - Q\left(\sqrt{\frac{2E_i}{N_o}}, \sqrt{\frac{2}{N_o}}\, x\right)\right) dx \qquad (2.50)$$

or normalizing with respect to signal-to-noise ratios, we have

$$P_{SE}(MOK) = 1 - 2r_1 e^{-r_1} \int_o^\infty y e^{-y^2 r_1} I_o(2yr_1) \prod_{i=2}^{M} \left(1-Q\left(\sqrt{2r_i}, \sqrt{2r_1}y \quad dy\right)\right) \qquad (2.51)$$

where $r_i = E_i/N_o$ and where the values E_i, i= 1, 2, 3, ..., M depend on the choice of the message waveforms.

In the following section, we will choose some specific signalling sets and evaluate their performance in the presence of doppler shift.

3.0 CHOOSING SIGNAL SETS FOR MOK

The choice of the orthogonal signal set for the MOK data modulation technique becomes important when there is relative motion (doppler shift) between the transponder and interrogator. At zero doppler shift the choice of the orthogonal set is not important (from the viewpoint of performance) since the outputs of the M-1 not true matched filters will be zero.

When there is relative motion between the interrogator and transponder, the choice of the orthogonal signal set determines the effective signal energy at the outputs of the M-1 not true matched filters. An ideal signal set would remain orthogonal for all doppler shifts (zero effective energy at the not true filter outputs).

Notice that regardless of the choice of the signal sets, the effective energy out of the true matched filter is

$$E_T = E_s \, \mathrm{sinc}^2 \, \omega_d T/2 \qquad (3.1)$$

where ω_d is the relative doppler frequency shift (in radians) between the received signal and the local receiver oscillator carrier frequencies.

Orthogonal waveform sets such as the Walsh functions are good candidates because they lend themselves to digital implementation. For instance, the M-ary signal set can be formed by selecting a single PN spread spectrum code and multiplying it by an appropriate set of M Walsh functions. The use of

Walsh functions also permits a single segmented convolver to perform the function of M matched filters.

The Walsh function sets can be generated by a set of orthogonal, antisymetric, square-wave basis functions known as the Rademacher functions. The first six Rademacher functions appear in Fig. 3.1, and can be represented by

$$R_n(t) = \begin{cases} \text{sign}\left[\sin\left(\frac{2^n \pi t}{T}\right)\right] & 0 \leq t \leq T \\ 0 & \text{Otherwise} \end{cases} \qquad (3.2)$$

where T is the data symbol duration. These functions form an incomplete set, but can be used to generate a complete set, the Walsh functions.

The first 22 Walsh Functions are shown in Fig. 3.2 The Walsh functions can be formed by considering all distinct combinations of products of the Rademacher functions. For instance, the first four Walsh functions $W_i(t)$, i=0,1,2 and 3 can be found by forming all distinct combinations of products of $R_1(t)$ and $R_1(t)$. $R_0(t)$ naturally arises as the identify element. That is,

$$\begin{aligned} W_0(t) &= R_0(t) \\ W_1(t) &= R_1(t) \\ W_2(t) &= R_1(t)R_2(t) \\ W_3(t) &= R_2(t) \end{aligned} \qquad (3.3)$$

where $R_i(t)R_i(t) = R_0(t)$ for any i.

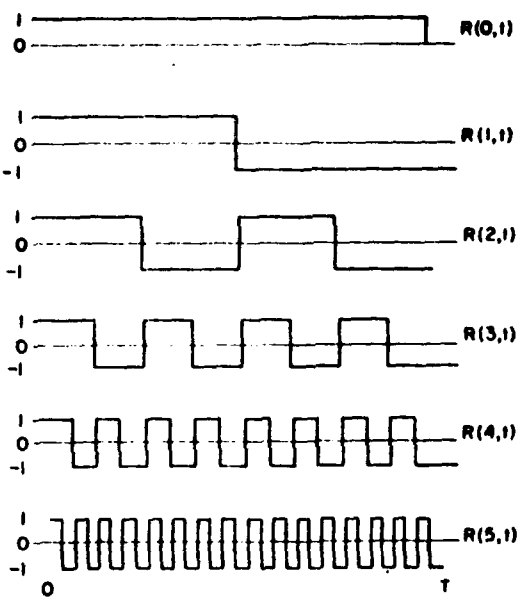

Fig. 3.1. A set of Rademacher functions.

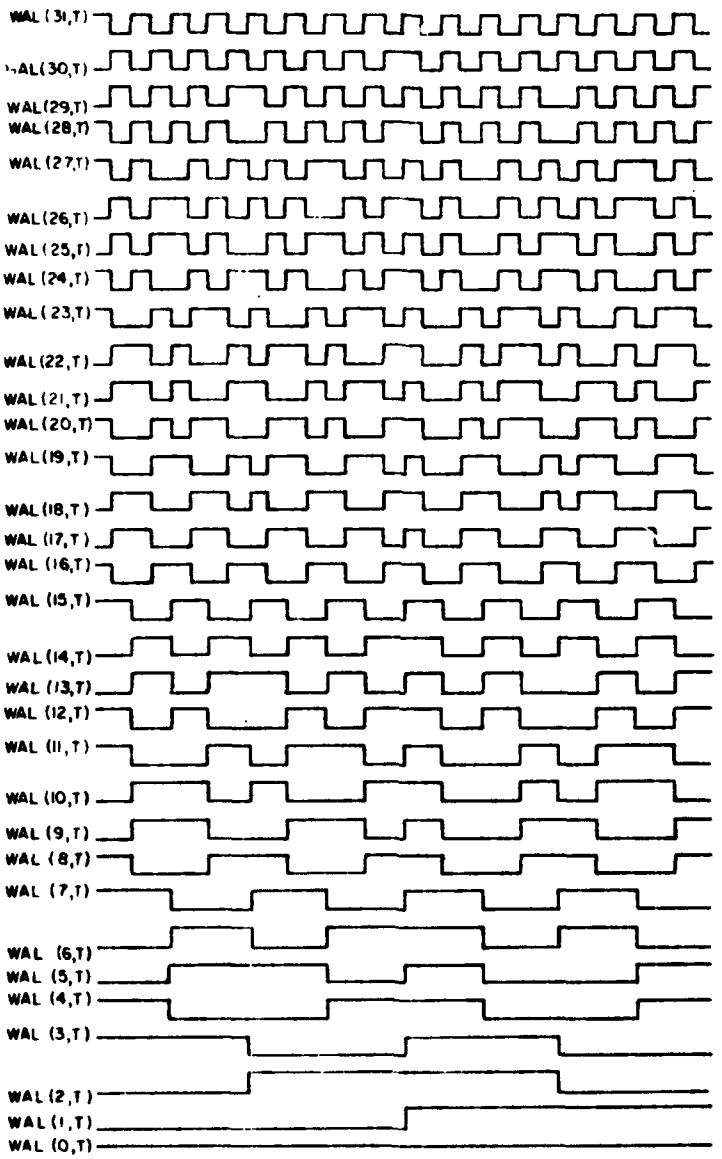

Fig. 3.2. A set of Walsh functions arranged in sequency order.

Similarly, the first eight Walsh functions can be formed from all distinct combinations of products of $R_1(t)$, $R_2(t)$ and $R_3(t)$. We have

$$\begin{aligned} W_0(t) &= R_0(t) \\ W_1(t) &= R_1(t) \\ W_2(t) &= R_1(t)\, R_2(t) \\ W_3(t) &= R_2(t)\, R_2(t) \\ W_4(t) &= R_1(t)\, R_3(t) \\ W_5(t) &= R_1(t)\, R_2(t)\, R_3(t) \\ W_6(t) &= R_2(t)\, R_3(t) \\ W_7(t) &= R_3(t) \end{aligned} \tag{3.4}$$

The Walsh function sets defined in this manner form a group under multiplication. Notice that the multiplication of any two Walsh functions in the set yields another member of the set. This property guarantees symmetry in that the probability of a symbol error is the same regardless of which symbol is sent.

By choosing higher frequency basis or Rademacher functions, the Walsh function sets will have better doppler performance. For example, suppose the 8-ary signal set is formed by all distinct combinations of products of $R_2(t)$, $R_3(t)$ and $R_4(t)$. This alternate Walsh function signal set becomes

$$
\begin{aligned}
W_0(t) &= R_0(t) \\
W_3(t) &= R_2(t) \\
W_4(t) &= R_2(t)\, R_3(t) \\
W_7(t) &= R_3(t) \\
W_8(t) &= R_3(t)\, R_4(t) \\
W_{11}(t) &= R_2(t)\, R_3(t)\, R_4(t) \\
W_{12}(t) &= R_2(t)\, R_4(t) \\
W_{15}(t) &= R_4(t)
\end{aligned}
\tag{3.5}
$$

The doppler performance of a particular Walsh function signal set is limited by the lowest frequency Rademacher function (excluding the identity function $R_0(t)$); in this case, $R_2(t)$.

The error performance in the presence of doppler shift of a particular signal set is given by Eq. 2.50 where the values E_i, i=2,3,...M are determined the choice of the signal set.

In general, the effective energy out of the i^{th} not true matched filter, which is matched to the ℓ^{th} Walsh function, given that the received signal is phase modulated by the r^{th} Walsh function is

$$
E_i = E_s \left| \frac{1}{T} \int_0^T W\ell(\lambda)\, W_r(\lambda)\, e^{j\omega_d \lambda}\, d\lambda \right|^2 \quad . \tag{3.6}
$$

The doppler performance of ideal BOK and sum-difference BOK where the signal set consists of the lowest order Walsh functions $W_0(t)$ and $W_1(t)$ is compared against that of QDPSK and DPSK in Fig. 3.3 Notice that the amount of improvement that is possible between sum-difference BOK and ideal BOK (about 3 dB at $\omega_d T = 1.5$). Thus, proper choice of the signalling set is important.

The MOK, M=4 probability of a symbol error is plotted in Fig. 3.4 versus doppler frequency shift for several symbol signal-to-noise ratios using the 4-ary signal set defined by Eq. 3.3. This signal set consists of the first four natural Walsh functions.

Similarly, the MOK, M=8 probability of a symbol error is plotted in Figs. 3.5, 3.6 and 3.7 versus doppler frequency shift for several symbol signal-to-noise ratios using the 8-ary signal set defined by Eq. 3.4, the alternate 8-ary signal set defined by Eq. 3.5 and the ideal 8-ary signal set (orthogonal for all doppler shifts), respectively.

The three 8-ary signalling sets are more clearly compared in Fig. 3.8 where the signal-to-noise ratio per bit required in order to maintain a 1% symbol error probability is plotted versus doppler shift for each of the three signal sets. We see that at $\omega_d T = 2$, the alternate signal set performs over 3 dB better than the low order Walsh function set.

Finally, in Fig. 3.9 the doppler performance of MOK for each value of M = 2, 4, 8 and 16 is compared for a signal set consisting of the first M

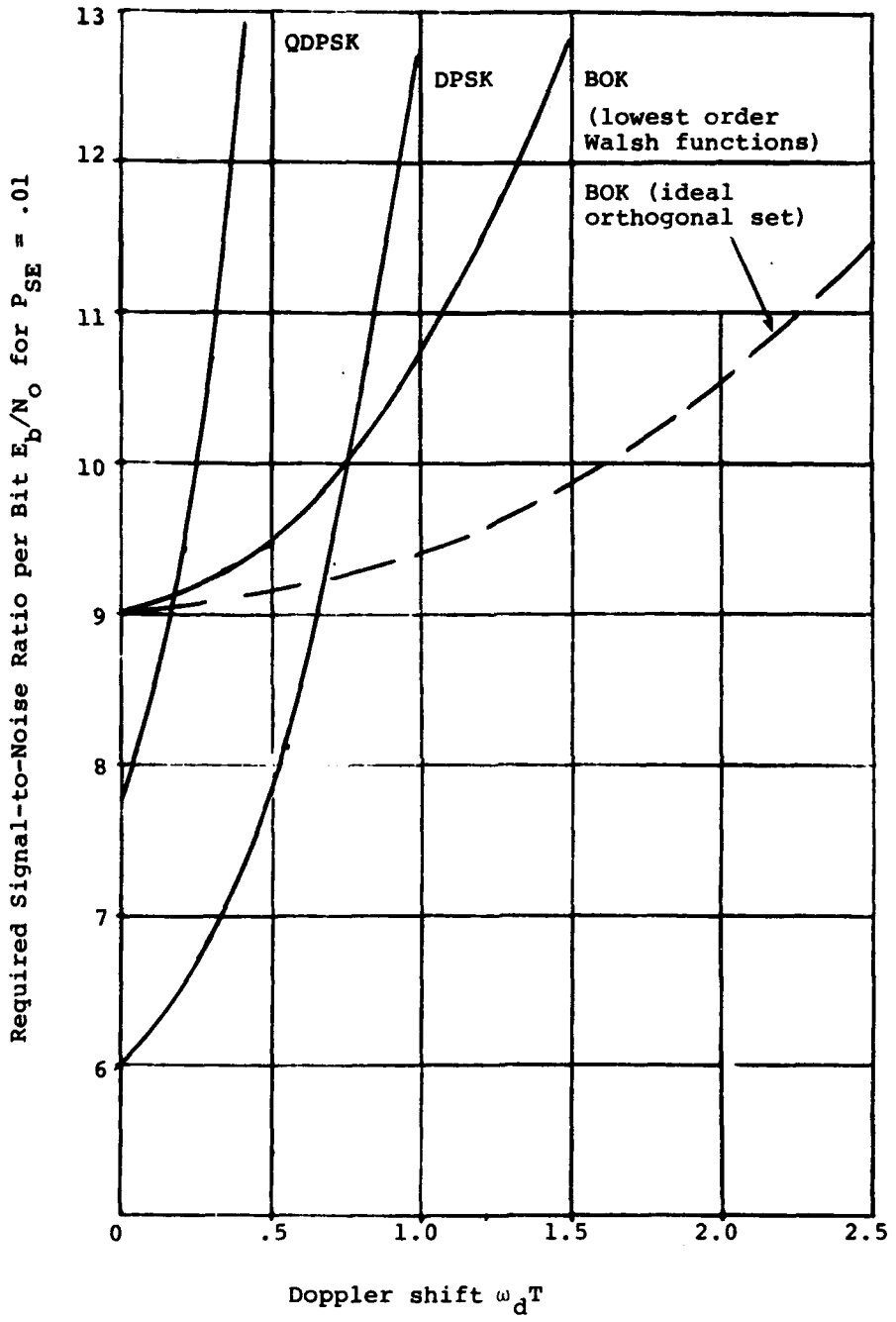

Fig. 3.3. Doppler performance of several modulation schemes.

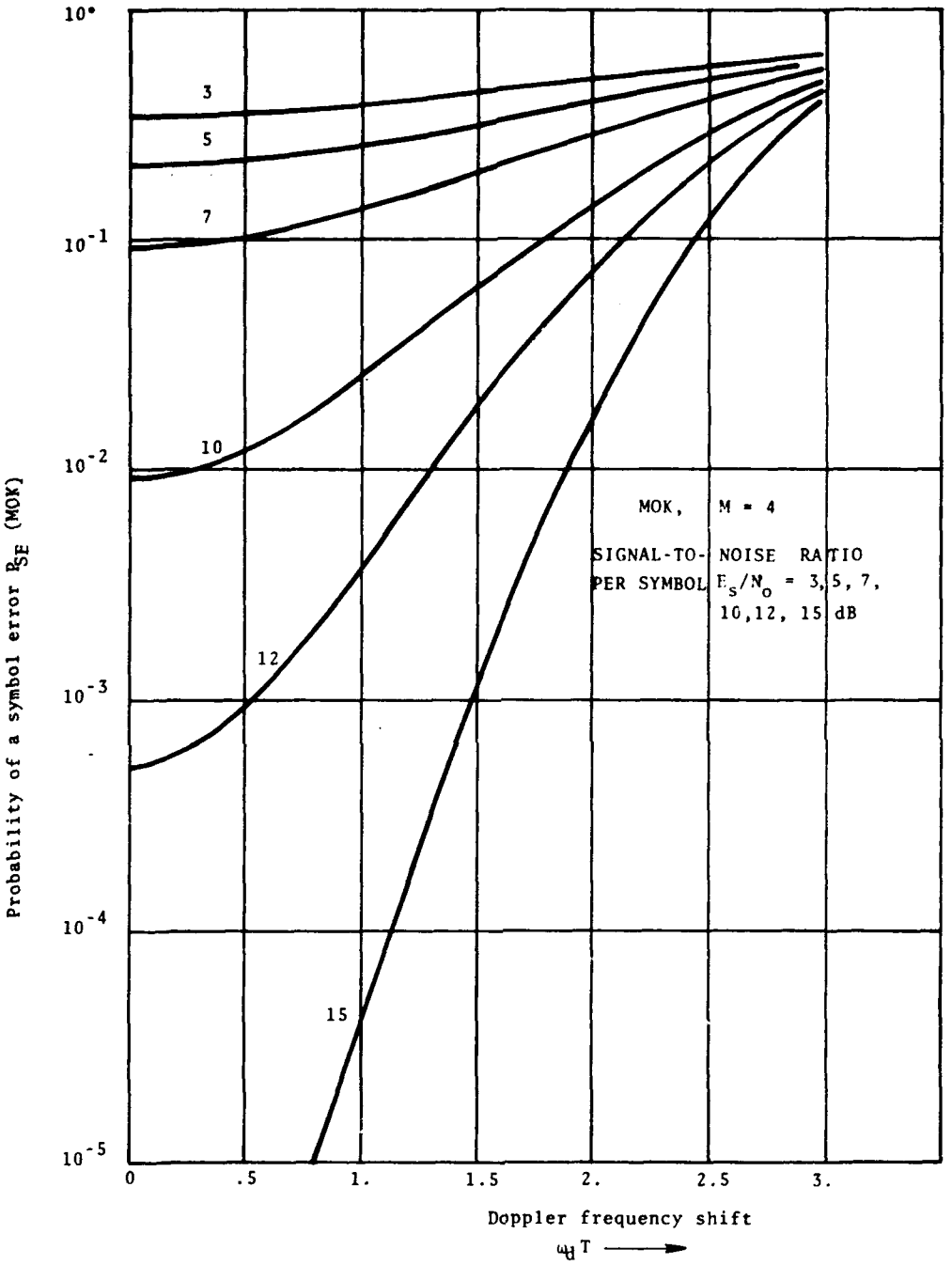

Fig. 3.4. Probability of a symbol error versus doppler shift for MOK, M = 4.

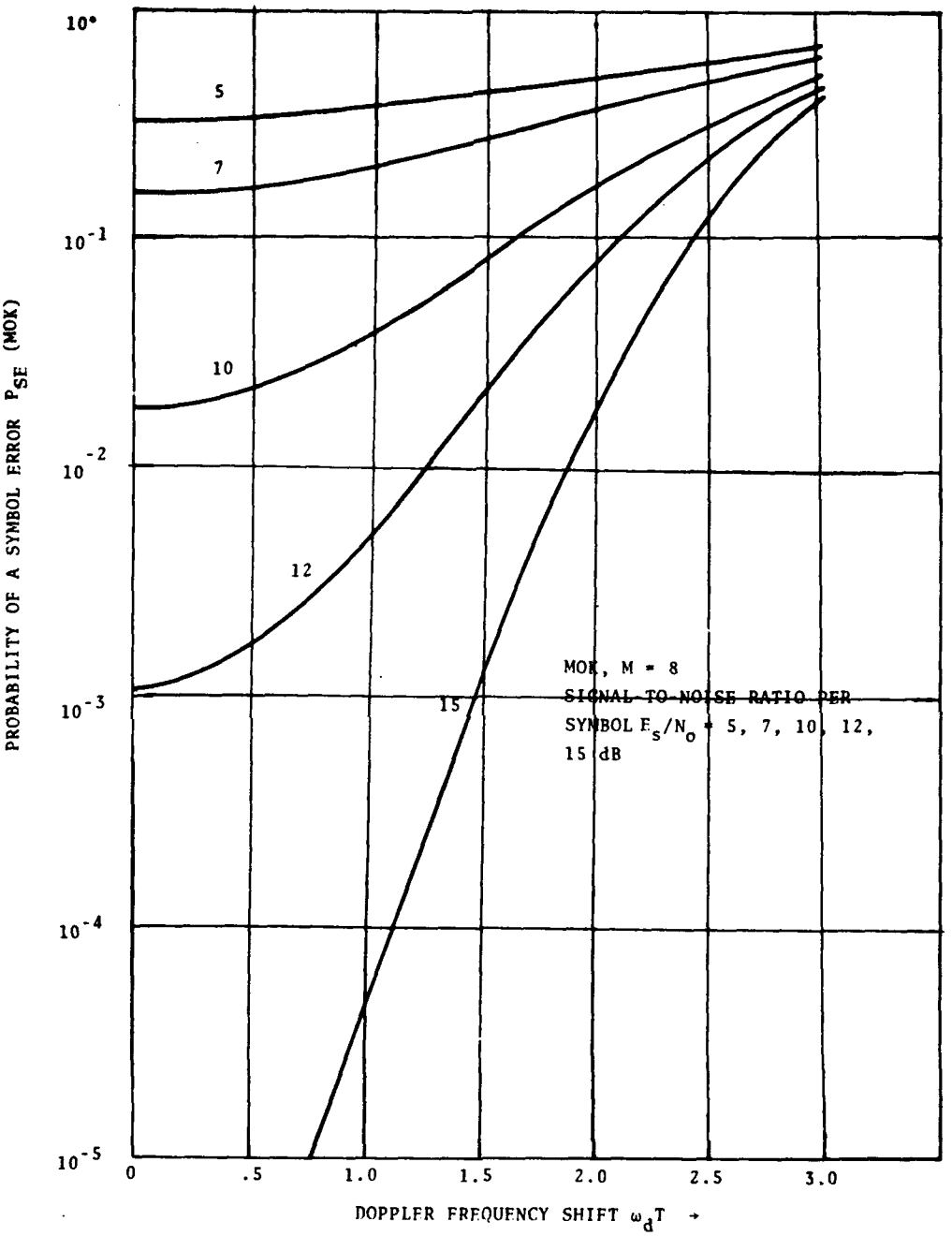

Fig. 3.5. Probability of a symbol error versus doppler frequency shift.

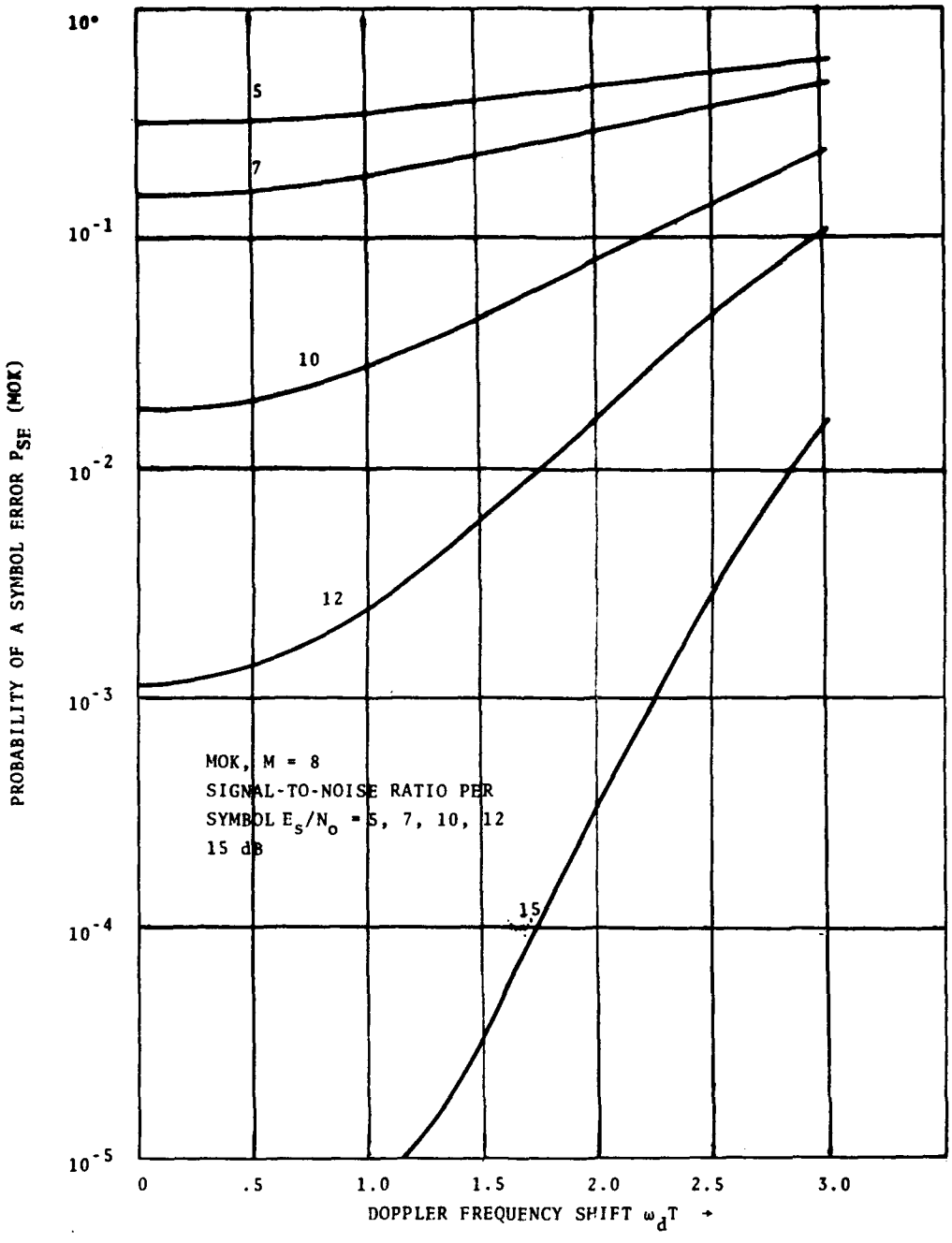

Fig. 3.6. Probability of a symbol error versus doppler frequency shift (phase waveforms chosen to be more doppler insensitive).

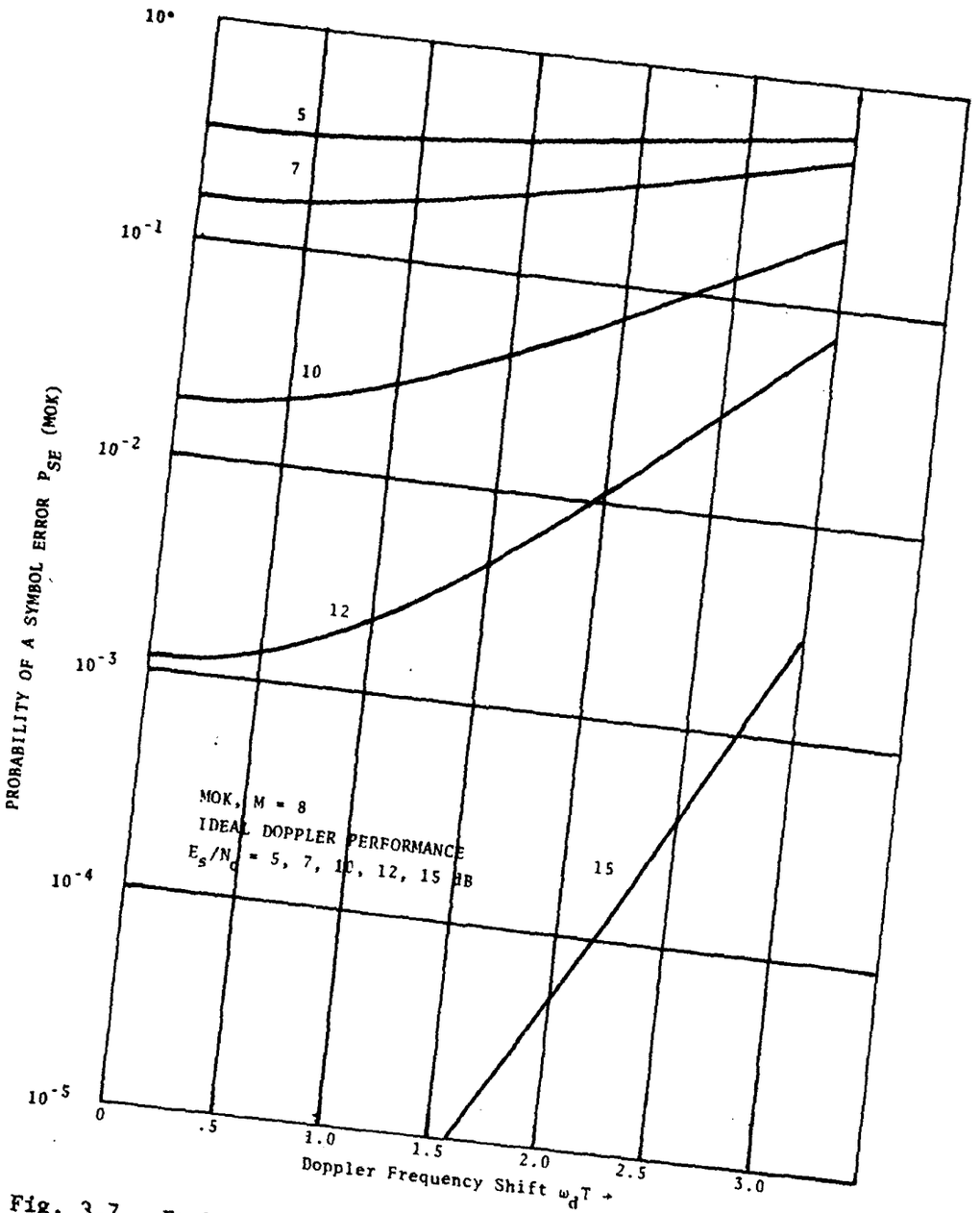

Fig. 3.7. Probability of a symbol error versus doppler frequency shift for ideal phase waveforms.

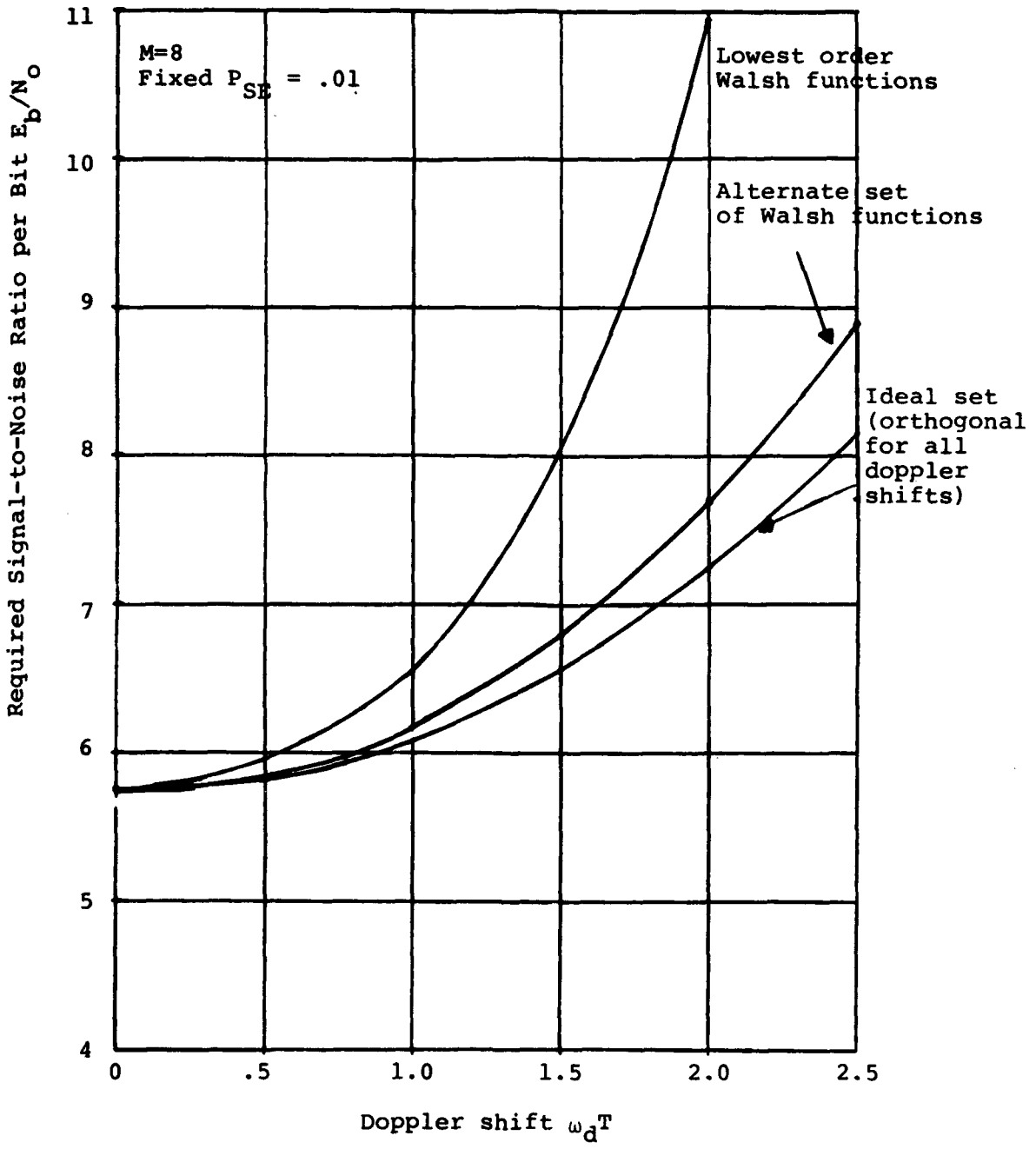

Fig. 3.8. Doppler performance for alternate signal sets, M = 8.

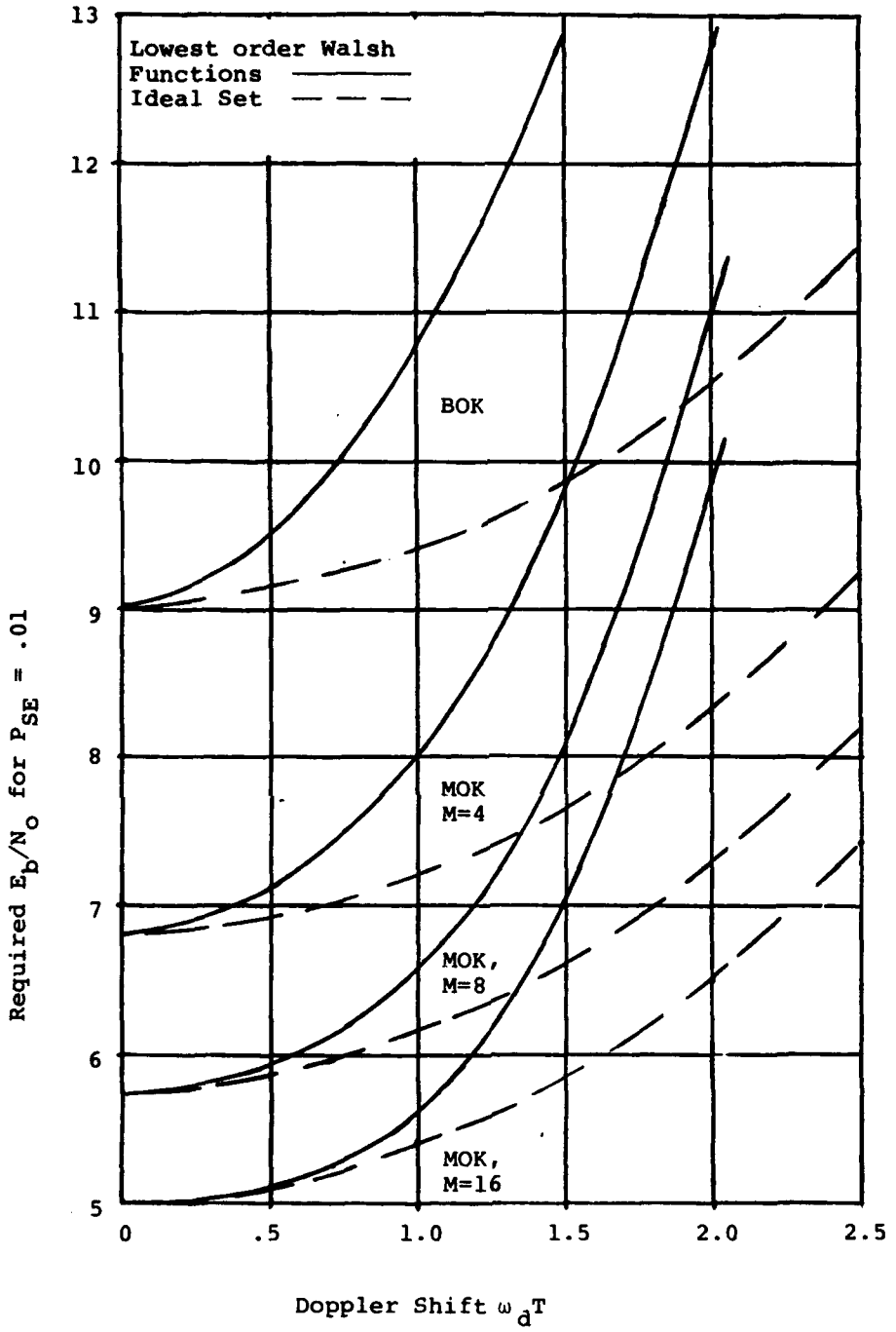

Fig. 3.9. Doppler performance of MOK, M = 2, 4, 8 and 16 for a fixed symbol error probability.

functions and for an ideal (orthogonal for all doppler shifts) M-ary signal set. Again, the signal-to-noise ratio per bit required to maintain a 1% symbol error probability is plotted versus doppler shift for each of the M-ary signal sets.

3.1 Signal Sets for BOK (MOK, M=2)

Of course, the binary signalling set is included in the previous discussion of MOK signalling sets. However, since the signal set is comprised of only two orthogonal signals, there are more options available. For instance, there is always the option that two independent PN chipping sequences be used for each data symbol. This would allow essentially ideal BOK performance (i.e., waveforms remain orthogonal for all doppler shifts of interest).

If a single PN chipping sequence is to be used, then the previous Walsh (Rademacher) function approach would dictate that the two phase waveforms be $R_0(t)$ and $R_j(t)$ where $j > 1$. In order to minimize the doppler degradation, j should be chosen as large as possible.

Suppose the signal set consists of $\theta_1(t) = R_0(t)$ and $\theta_2(t) = R_j(t)$ where $j = \log_2 N$ as shown in Fig. 3.1.

Consider the response of the filter matched to $\theta_2(t)$ when $\theta_1(t)$ is sent. After demodulation with respect to the PN chip sequence and the data $\theta_1(t)$, the matched filter output at the sample time t_s becomes (noiseless case)

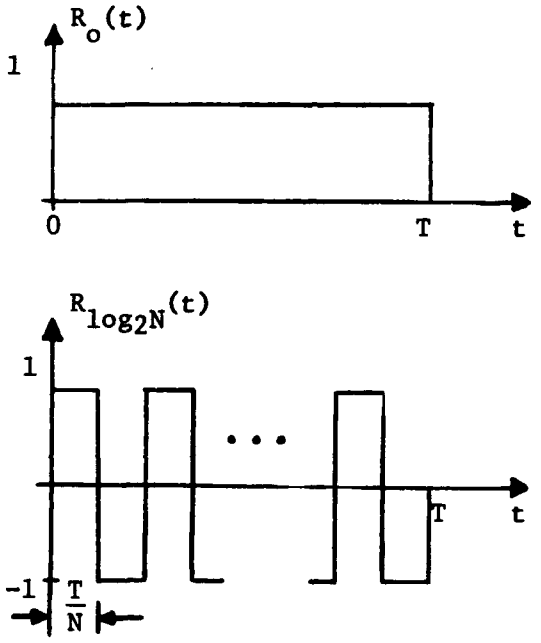

Fig. 3.10. Signal set for BOK.

$$y_o(t_s) = \frac{\sqrt{E_s}}{T} \sum_{i=0}^{N-1} (-1)^i \int_{iT/N}^{(i+1)T/N} e^{j\omega_d t}\, dt$$

$$= \frac{\sqrt{E_s}}{N} \operatorname{sinc}\left(\frac{\omega_d T}{2N}\right) e^{j\omega_d T/2N} \sum_{i=0}^{N-1} (-1)\, e^{j\omega_d T i/N} \quad . \tag{3.7}$$

The output of the envelope detector becomes

$$|y_o(t_s)| = \frac{\sqrt{E_s}}{N} \left|\operatorname{sinc} \frac{\omega_d T}{2N}\right| \sqrt{N + 2 \sum_{i=1}^{N-1} (N-i)(-1)^i \cos \frac{\omega_d T}{N}} \quad . \tag{3.8}$$

It can be shown (see Appendix A) that in the limit as $N \to \infty$ the response of the not true filter (3.8) approaches zero. As a practical limit, N can be made as large as the number of chips per data symbol. For values of N much greater than 16 (see Fig. 3.11), the response of the not true filter is essentially zero for realistic doppler shifts.

Thus, by choosing a waveform $\theta_2(t)$ with a large enough value of N, the waveforms maintain orthogonality regardless of the doppler shift. Of course, remember that the effective energy out of the true channel matched filter is

$$E' = E_s \operatorname{sinc}^2 \omega_d T/2 \quad . \tag{3.9}$$

The effective energies out of the true matched filter and the not true matched filter are plotted in Fig. 3.11 as a function of the doppler shift for several values of N. Notice that the effective energy out of the not true filter is just the square of (3.8) with $E_s = 1$.

For large N the performance of this BOK scheme can be found by using the original zero doppler probability of error curves where E_s is replaced by E' (see Fig. 2.5 of Section 2.2).

The question remains as to whether the waveform $R_j(t)$ can be implemented for large values of j. It if adds too much complexity to the matched filter, then an alternative waveform must be chosen.

An alternative choice of the second BOK signal $\theta_2(t)$ is given in Fig. 3.12.

The idea is to choose k in such a way that the doppler degradation is minimized.

Consider the response of the filter matched to $\theta_2(t)$ when $\theta_1(t)$ is sent. The matched filter output at the sample time t_s becomes (noiseless case)

$$y_o(t_s) = \frac{\sqrt{E_s}}{T}\left(\int_0^{T(1-k)/2} e^{j\omega_d t}\,dt - \int_{T(1-k)/2}^{T(1+k)/2} e^{j\omega_d t}\,dt + \int_{T(1+k)/2}^{T} e^{j\omega_d t}\,dt\right)$$

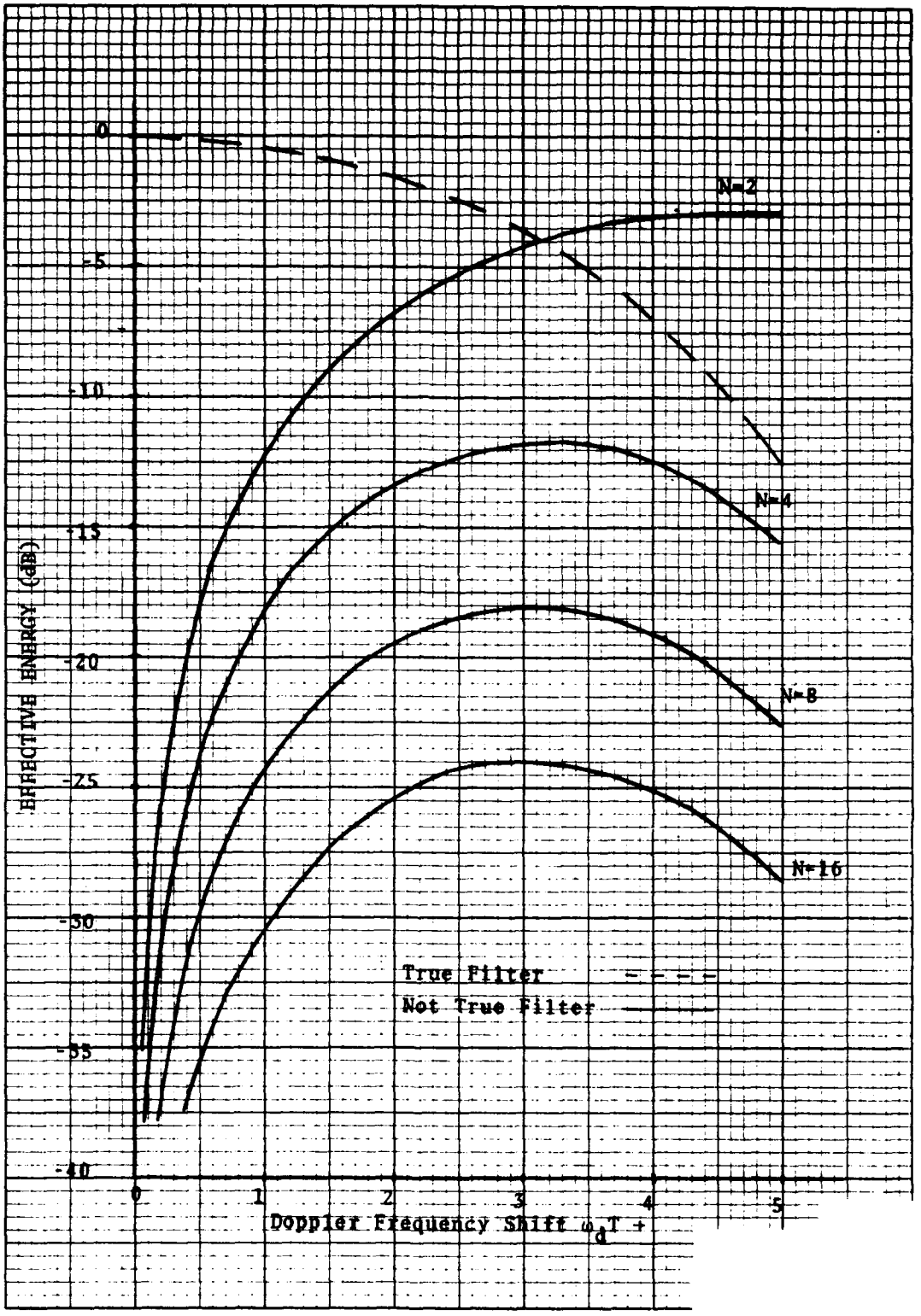

Fig. 3.11. Effective energy versus doppler frequency shift with $E_s = 1$ for BOK.

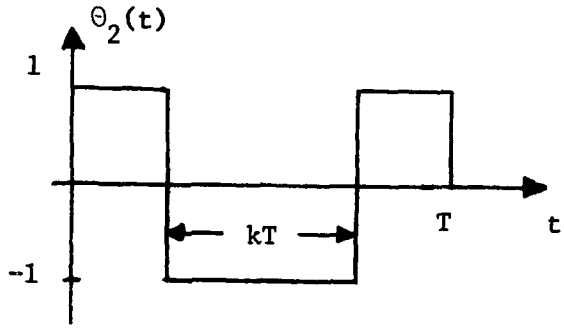

Fig. 3.12. Alternative choice for $\theta_2(t)$.

$$= \sqrt{E_s}\ \frac{(1-k)}{2}\ \text{sinc}\phi(1-k)\ \left[e^{j\phi(1-k)} + e^{j\phi(3+k)}\right]$$

$$- \sqrt{E_s}\ \frac{k}{2}\ \text{sinc}\phi k\ \left[e^{j\phi(2-k)} + e^{j\phi(2+k)}\right] \qquad (3.10)$$

where $\phi = \omega_d T/4$.

After some manipulation, we see that the matched filter output (3.10) will be zero is k is given by the optimum value

$$k^* = \frac{1}{2\phi}\ \sin^{-1}\left(\frac{\sin 2\phi}{2}\right)$$

$$= \frac{2}{\omega_d T}\ \sin^{-1}\left(\frac{\sin\ \omega_d T/2}{2}\right) \qquad (3.11)$$

The optimum value k* is plotted in Fig. 3.13 as a function of the doppler frequency shift.

Unfortunately, the choice of k* guarantees orthogonality only at a particular doppler frequency shift. However, by identifying the range of possible doppler shifts, one can choose a value of k that minimizes (3.10) over the region of interest. For instance, if the worse case doppler shift corresponds to 2.5 radians, then a compromized value of k between .5 and .4 could be chosen.

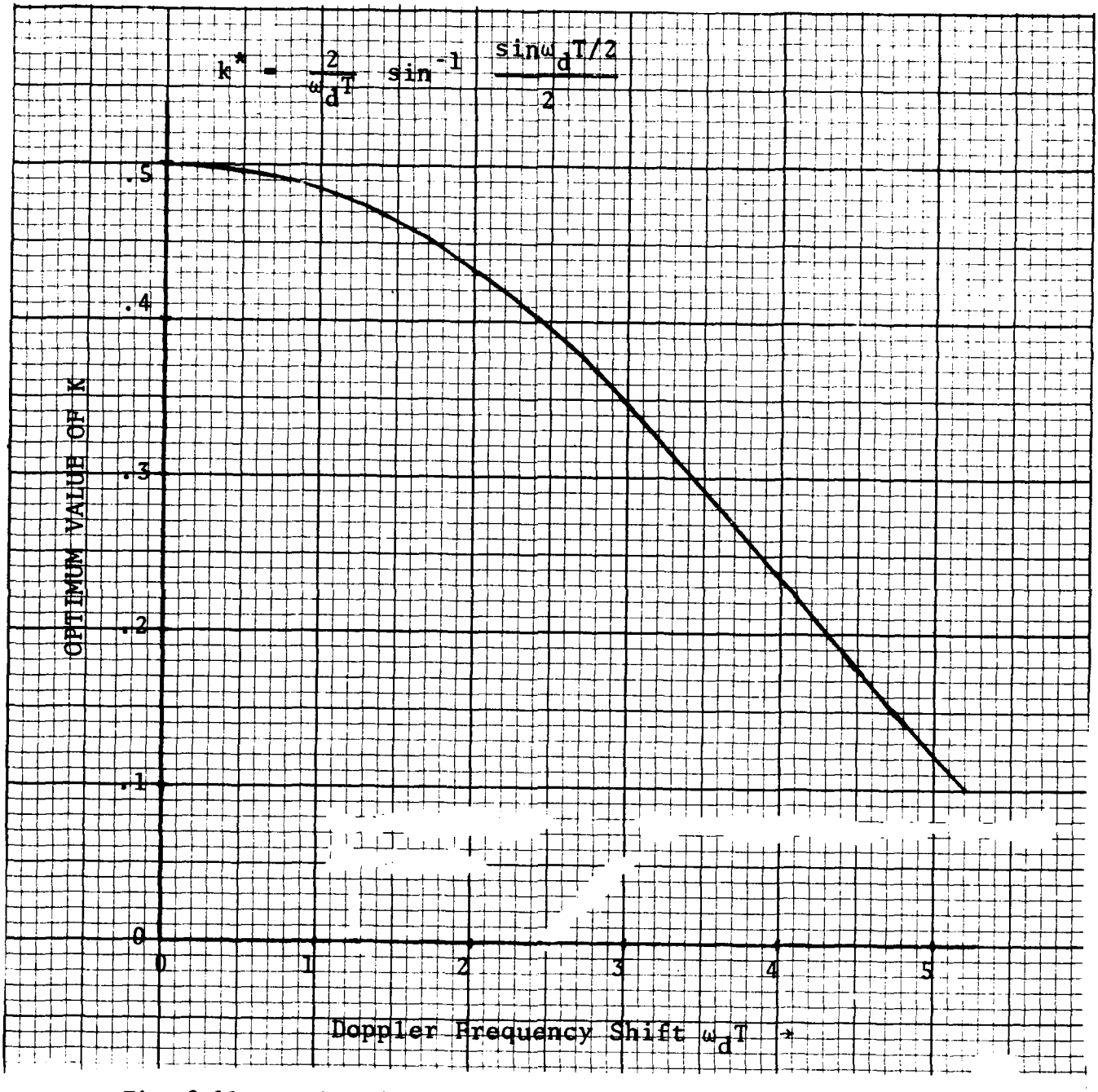

Fig. 3.13. Optimum k versus doppler frequency shift.

In Fig. 3.14, the effective energies out of the true and not true matched filters are plotted versus doppler shift for several values of k. The effective energies out of the not true filter for the signal set of Fig. 3.10 with N=2 and 4 are also plotted for comparison. Note that $0 < k < .5$ essentially offsets the null of the not true filter from zero doppler.

The relative performance of these special case BOK signal sets are shown in Fig. 3.15 where the signal-to-noise ratio per bit required in order to maintain a 1% symbol (bit) error probability is plotted versus doppler shift.

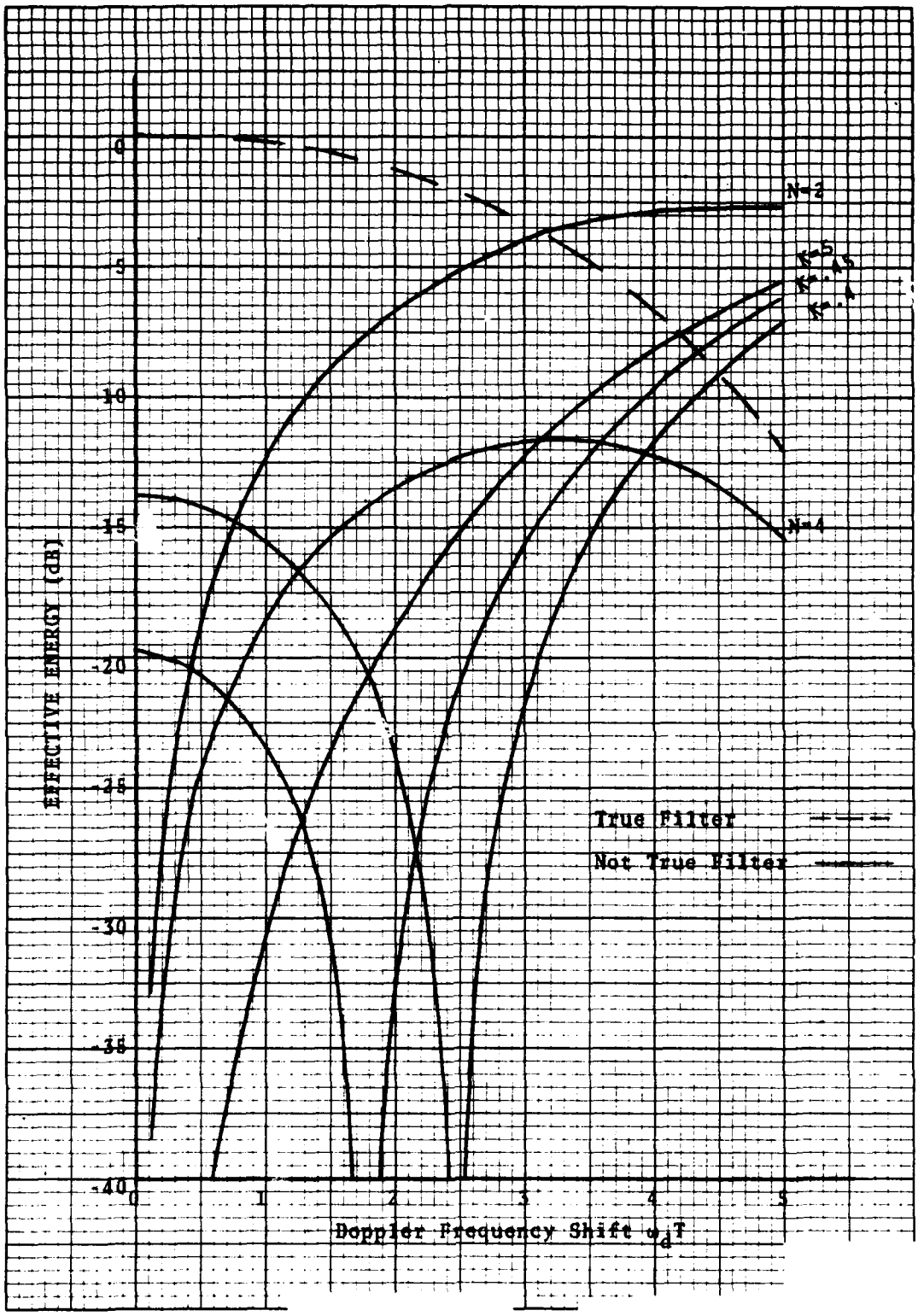

Fig. 3.14. Effective energy versus doppler frequency shift with E_s = 1 for special case BOK.

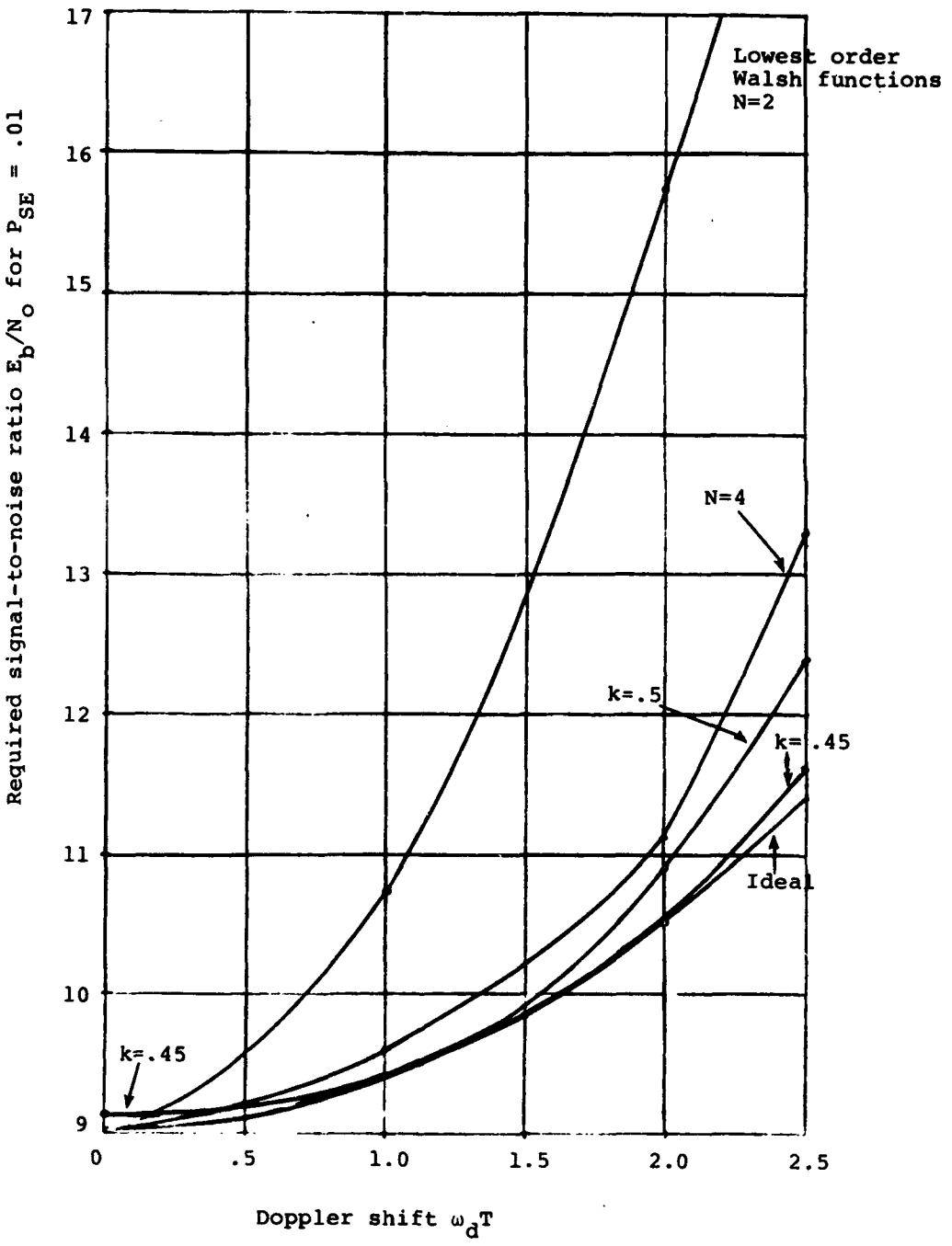

Fig. 3.15. Relative comparison of special case BOK.

4.0 ACOUSTO-ELECTRIC CONVOLVER IMPLEMENTATIONS

This section is devoted to acousto-electric convolver implementations of the various data modulation techniques under consideration. Implementation of MDPSK for M=2 and 4 is also presented here, although their doppler performance precludes them from serious consideration.

The structures of the convolver based receivers are of the matched filter/greatest of form (as shown in Fig. 2.4). A general M-ary convolver based receiver structure is given in Fig. 4.1 whereby the convolver and sum-difference hybrid matched filter connections will be supplied for each of the modulation schemes.

The convolver/sum-difference hybrid matched filters for DPSK and QDPSK are shown in Fig. 4.2 Notice that sum-difference BOK is implemented in the same manner as DPSK.

In Fig. 4.3, three possible signal sets for MOK, M=4 are shown. The three sets are formed by considering all possible distinct multiplicative combinations of (a) $R_0(t)$, $R_1(t)$ and $R_2(t)$, (b) $R_0(t)$, $R_2(t)$ and $R_3(t)$, and (c) $R_0(t)$, $R_3(t)$ and $R_4(t)$. Remember that the sets formed from the higher order Rademacher functions will have better doppler performance.

As mentioned earlier, sum-difference BOK can be implemented with a two segment convolver and one sum-difference hybrid (this corresponds to a signal

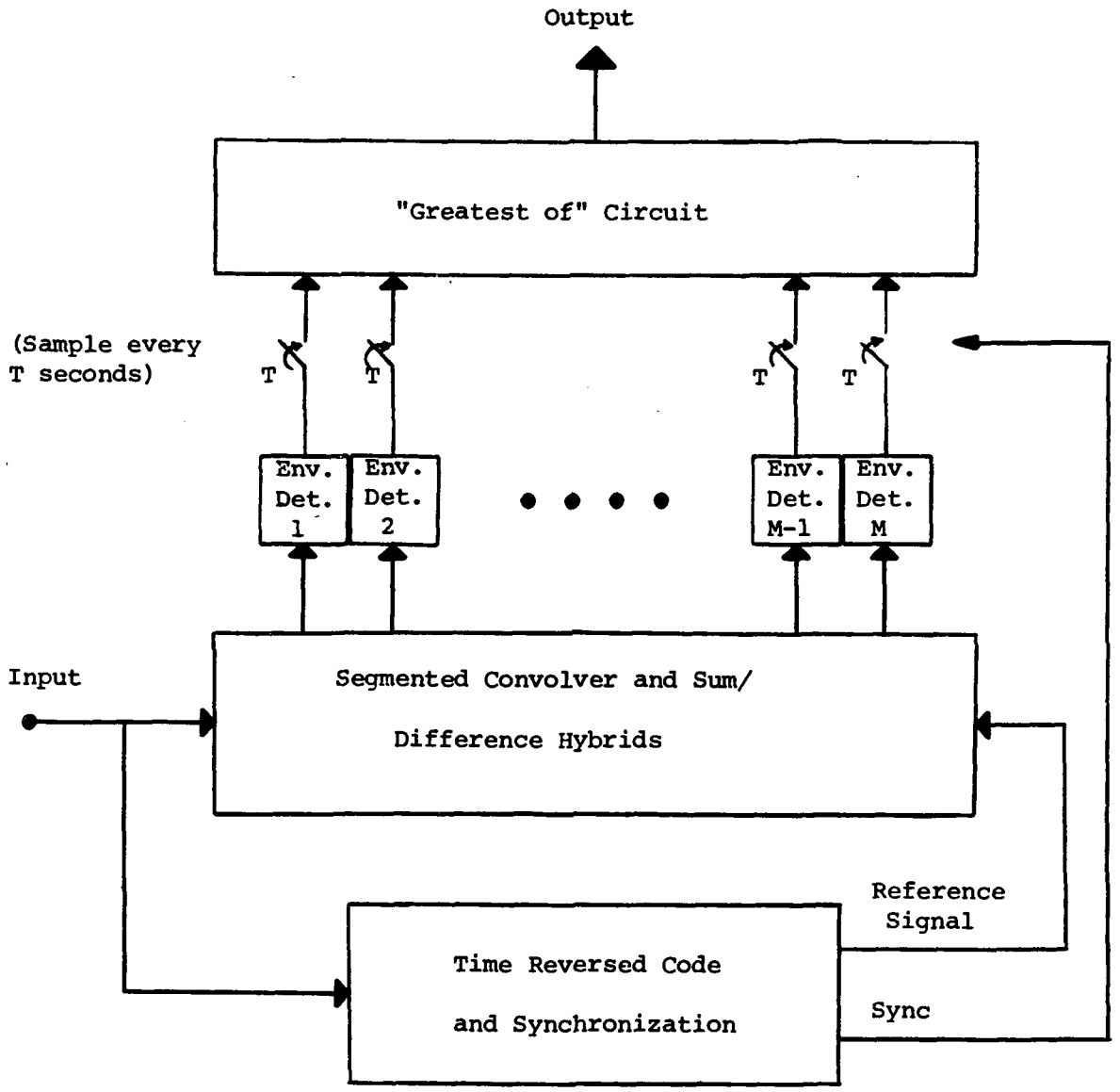

Fig. 4.1 General M-ary receiver block diagram

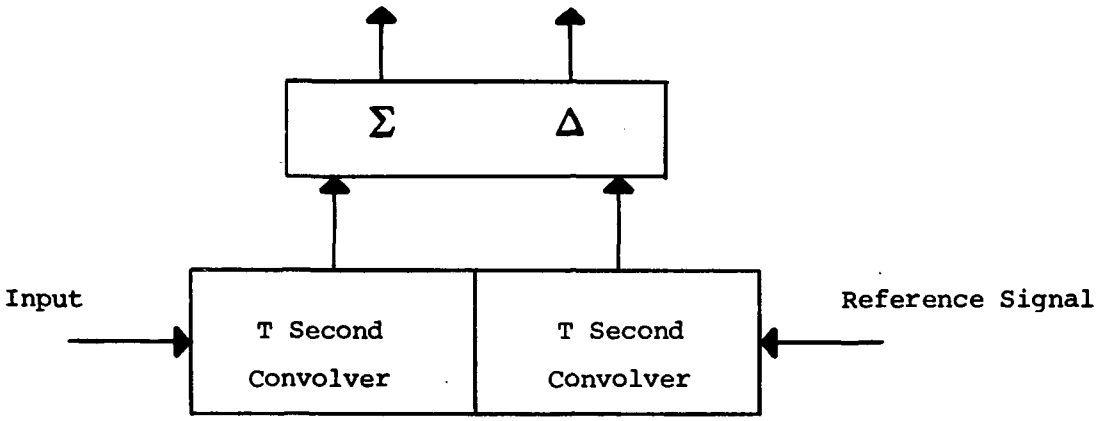

a) DPSK or sum/difference BOK with symbol length 2T

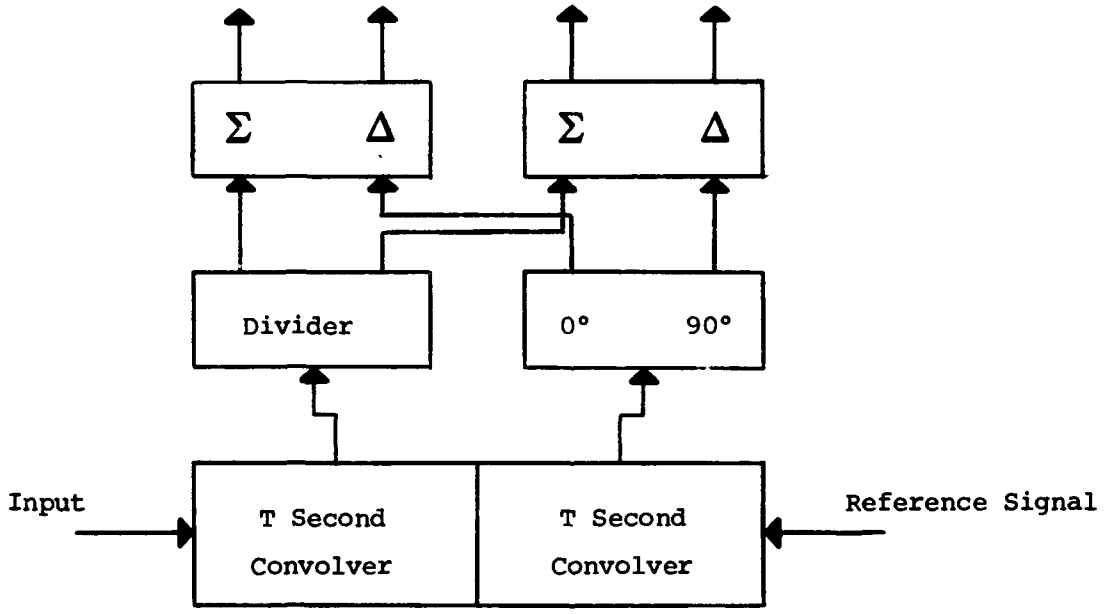

b) QDPSK

Fig. 4.2 Convolver matched filters for DPSK and QDPSK

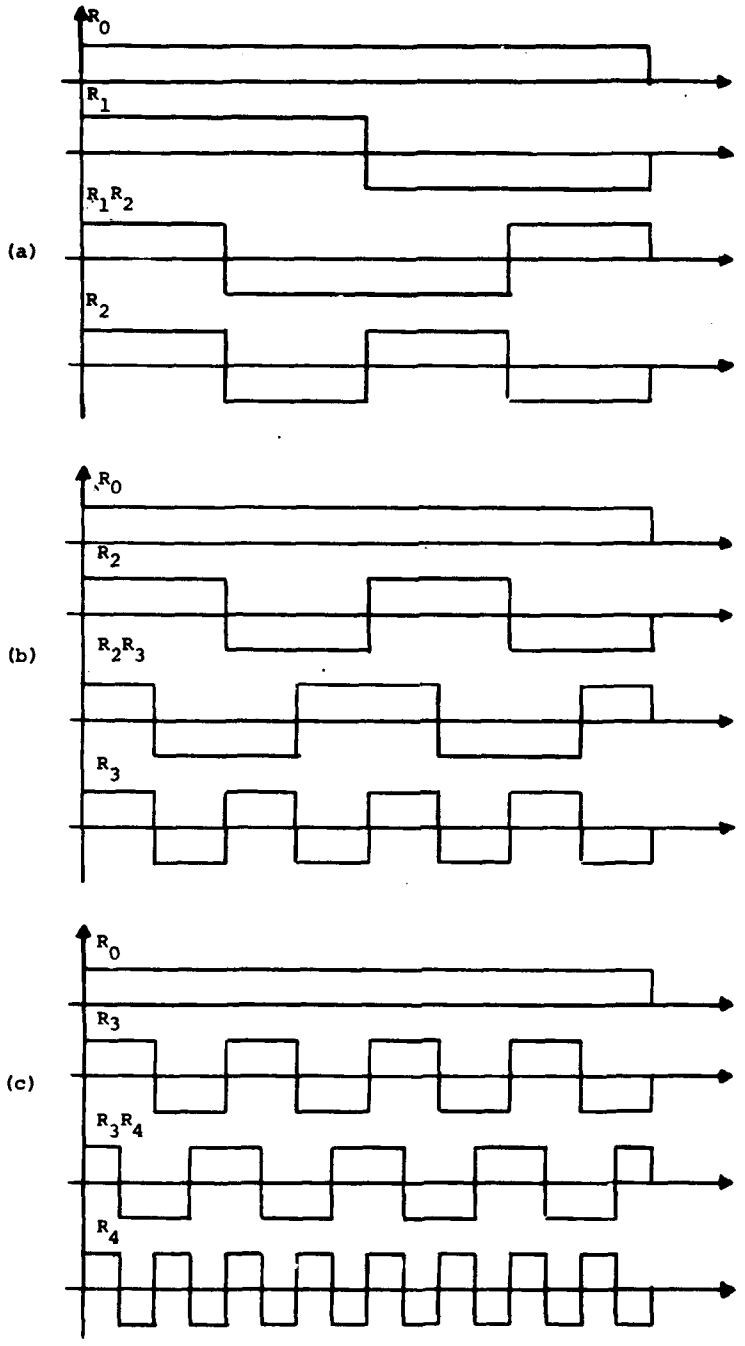

Fig. 4.3. Possible signal sets for MOK, M = 4. (a) First 4 Walsh functions. (b) All combinations of R_0, R_2 and R_3. (c) All combinations of R_0, R_3 and R_4.

set consisting of $R_0(t)$ and $R_1(t)$. Figure 4.4(a) shows a straightforward implementation of BOK, where the signal set consists of $R_0(t)$ and $R_2(t)$, using a single four segment convolver with four sum-difference hybrids.

Figure 4.4(b) shows an implementation of the 4-ary signal set given in Fig. 4.3(b) using a single eight segment convolver and 12 sum-difference hybrids.

In general, to implement an M-ary signal set with a single convolver we require at least an M segment convolver. If we choose to improve the doppler performance by choosing a signal set which requires 2^n, $n \geq 1$ times as many segments, then for an M-ary signal set we require

$$2^n M \tag{4.1}$$

segments. Using the straightforward implementation approach, we would require,

$$2^{n-1} M \log_2(2^n M) \tag{4.2}$$

sum-difference hybrids.

Assuming that we do not want to build 4-ary convolvers with more than 16 segments, then there are three possible choices for n, namely, n=0, 1 or 2.

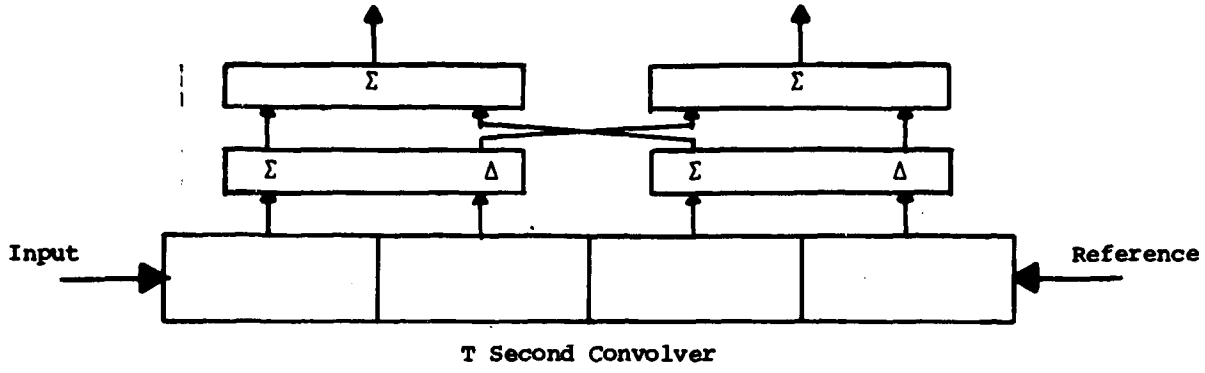

(a) Binary convolver matched to $R_0(t)$ and $R_2(t)$

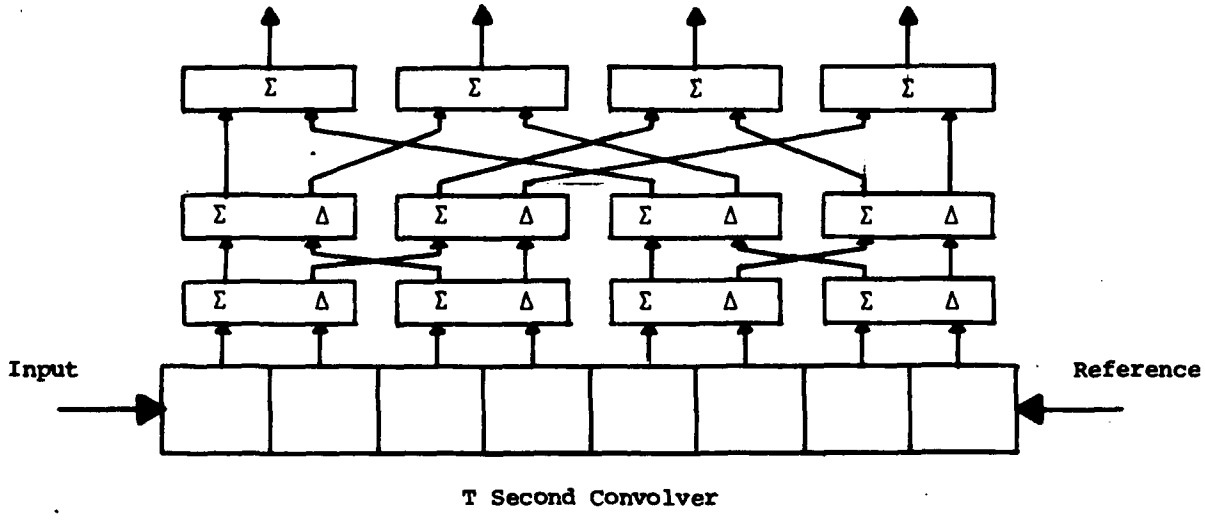

(b) 4-ary convolver matched to $R_0(t)$, $R_2(t)$, $R_2(t)R_3(t)$ and $R_3(t)$.

Fig. 4.4 Straightforward sum/difference hybrid implementation of segmented convolvers for enhanced doppler performance.

However, for n=1, there are 8 segments and by (4.2) we would need 12 sum/difference hybrids. Similarly, for n=2 there are 16 segments and by (4.2) we would need 32 sum/difference hybrids. Clearly, the number of sum/difference hybrids required becomes prohibitive. The following examples will illustrate an alternative approach.

Consider the original signal set shown in Fig. 4.3(a) which consists of all multiplicative products of the Rademacher functions R_0, R_1 and R_2. The corresponding standard 4-segment convolver implementation (n=0) is shown in Fig. 4.5(a).

Now consider the alternate signal set shown in Fig. 4.3(b) which consists of all products of R_0, R_2 and R_3. This signal set has much better doppler performance than the original set and requires an 8-segment convolver (n=1). However, by tieing appropriate segment pairs together we can implement this alternate signal set with only 4 sum/difference hybrids as shown in Fig. 4.5(b).

For even better doppler performance (close to ideal even at high band) this approach can be extended to the signal set which requires a 16-segment convolver (n=2). The waveform set is shown in Fig. 4.3(c) and consists of all multiplicative products of R_0, R_3 and R_4. By tieing together the appropriate groups of segments, we can implement this waveform set with only 4 sum/difference hybrids as shown in Fig. 4.5(c).

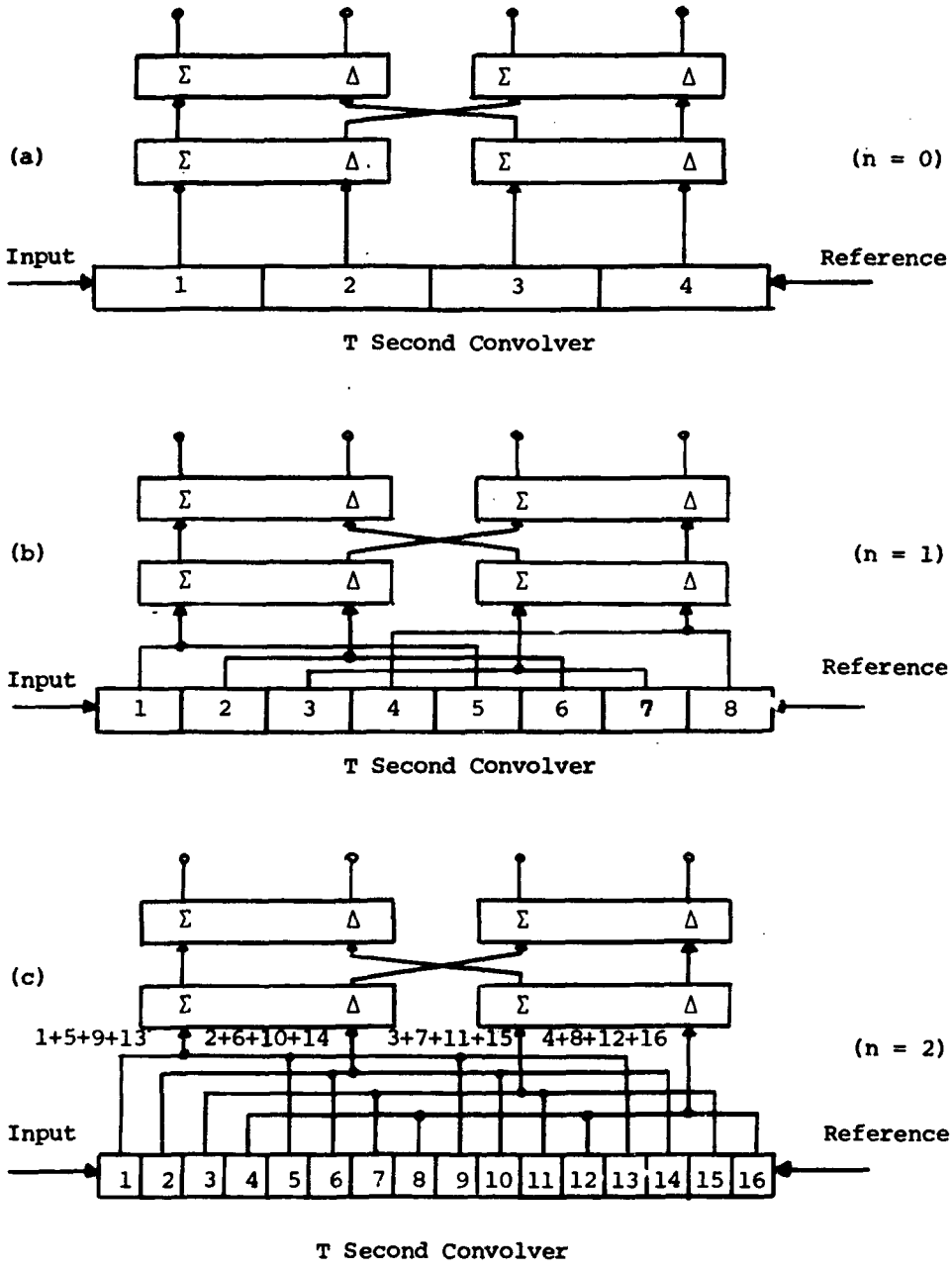

Fig. 4.5. Convolver implementations of the 4-ary signal sets of Fig. 4.3. (a) First four Walsh functions; (b) all combinations of R_0, R_2 and R_3; and (c) all combinations of R_0, R_3 and R_4.

Thus, in general we can implement an M-ary convolver which has $2^n M$ segments with $M/2 \log_2 M$ sum-difference hybrids.

Figure 4.6 shows three possible signal sets for BOK, including the original sum-difference set. The corresponding convolver implementations are shown in Fig. 4.7.

Finally, in Fig. 4.8 we show the construction of higher order M-ary convolver matched filters using n lower order $\frac{m}{n}$-ary convolver matched filters. Examples are shown for constructing a 4-ary or 8-ary matched filter using two binary or two 4-ary convolver matched filters, respectively, and for constructing a 8-ary or 16-ary matched filter using four binary or four 4-ary convolver matched filters, respectively. The reference modulating Rademacher functions R_j depend on the desired signal set and the number of segments per convolver.

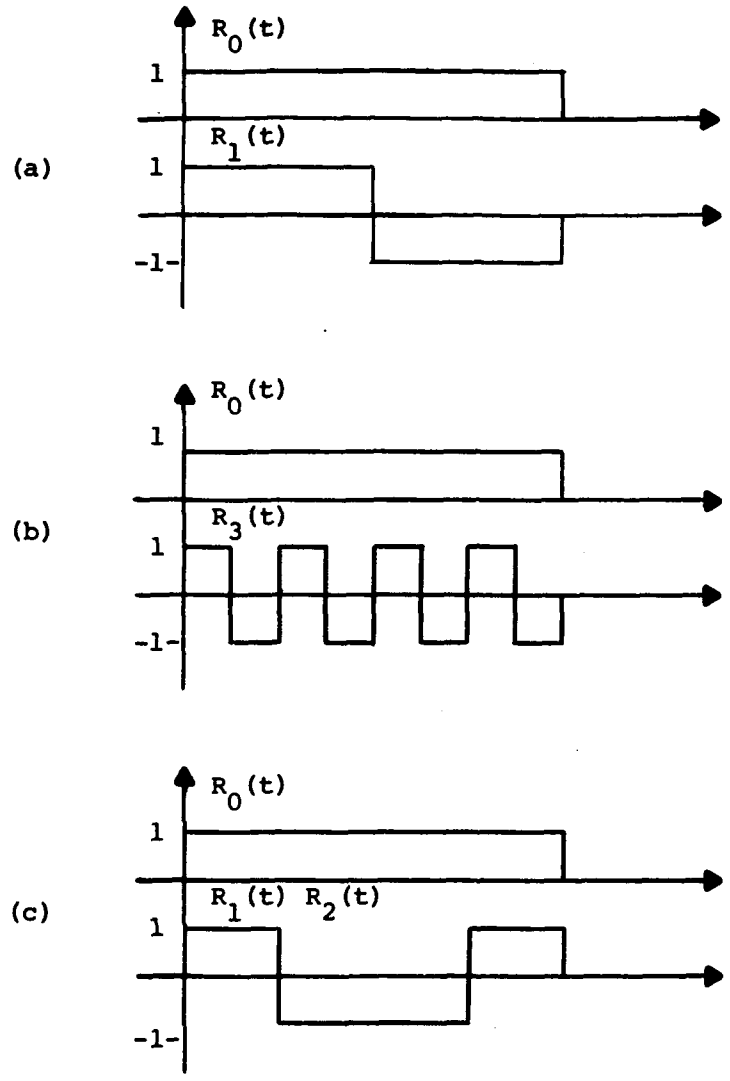

Fig. 4.6. Special waveforms for (a) sum/difference BOK, (b) eight segment BOK, and (c) special case BOK with k = 1/2.

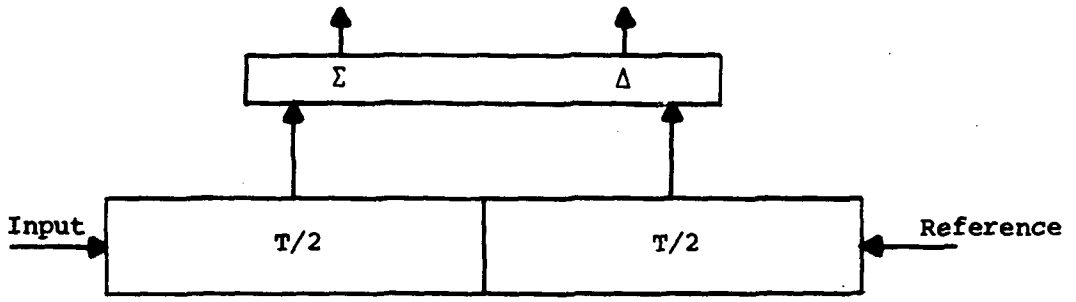

a) Sum/difference BOK

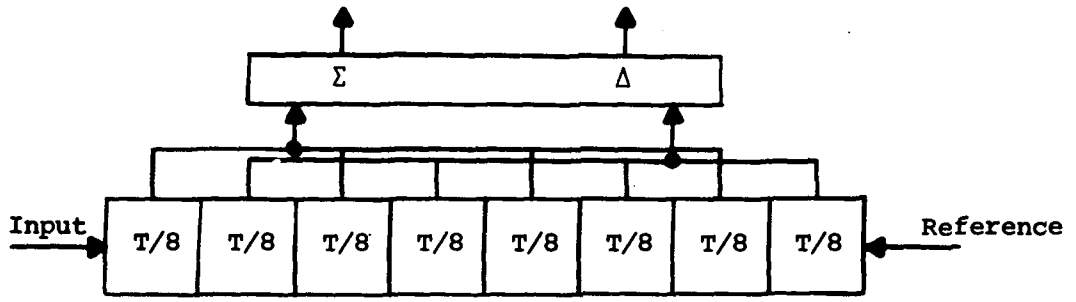

b) BOK, N = 8

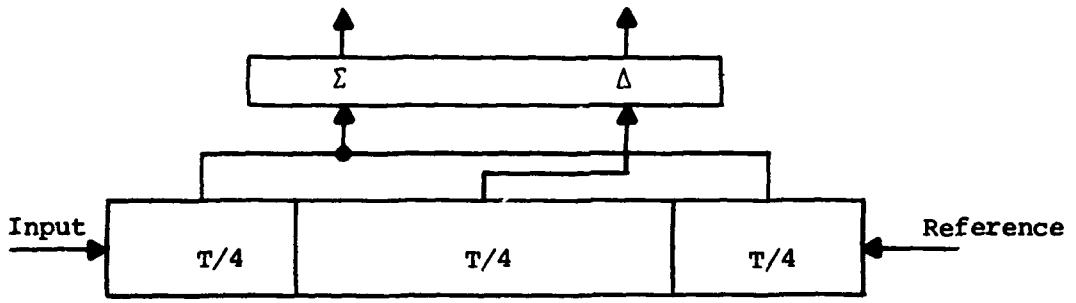

c) Special case BOK, k = 1/2

Fig. 4.7. Three segmented convolver matched filters for BOK using a single PN reference code.

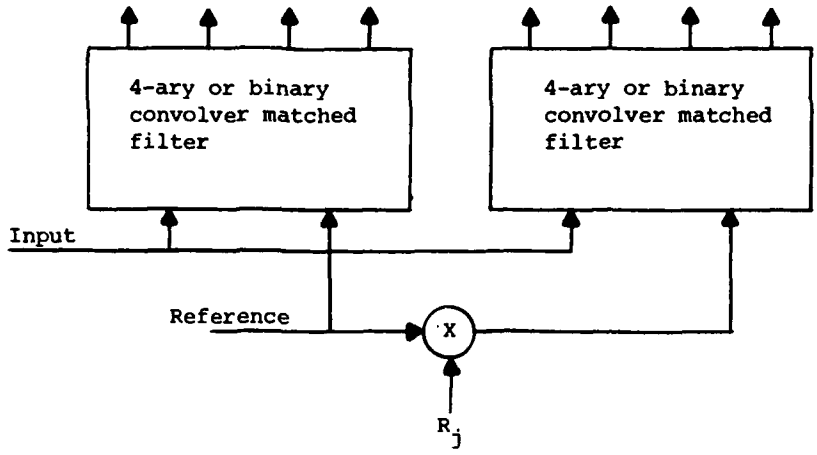

(a) 8-ary or 4-ary convolver matched filter from two 4-ary or two binary convolvers, respectively.

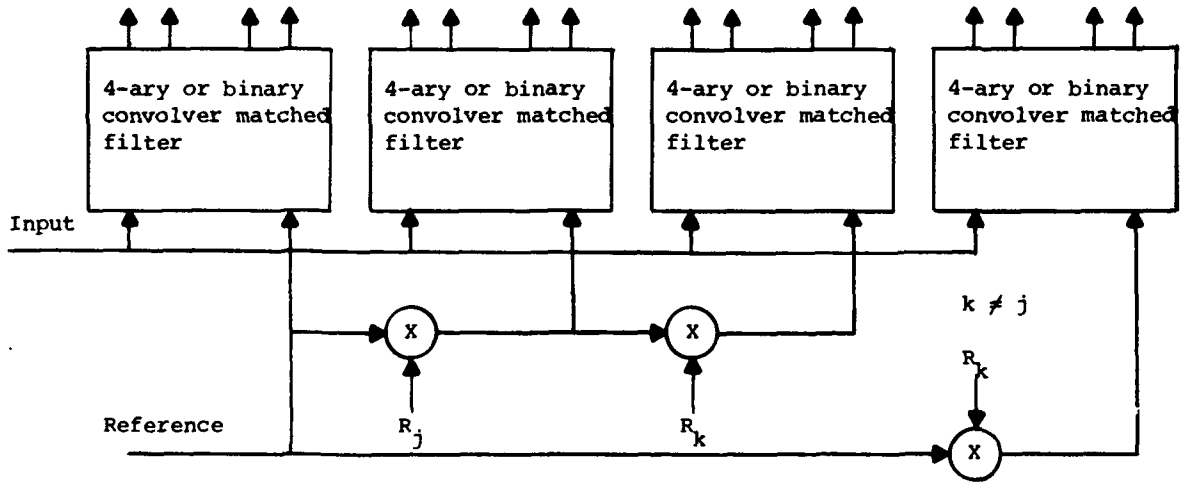

(b) 16-ary or 8-ary convolver matched filters from four 4-ary or four binary convolvers, respectively.

Fig. 4.8. Construction of higher order M-ary convolver matched filters using several binary or 4-ary convolvers.

5.0 RELATIVE COMPARISON OF MOK FOR M=2, 4, 8, 16 AND 32

This section makes a relative comparison of several data modulation schemes on the basis of the required energy per bit E_b and of the required time per bit T_b for a given message reliability. Specifically, a comparison of binary differential phase shift keying DPSK and M-ary incoherent orthogonal keying MOK for M = 2, 4, 8, 16 and 32 is made. Also, the performances of these modulation schemes are compared for two fixed values of carrier frequency doppler shift in terms of the choice of the message waveforms. As in the previous memos, the transmitted signals are assumed to be corrupted only by white Gaussian noise of two sided spectral density No/2 watts/Hz.

In order to compare the doppler performance of DPSK on an equal basis with that of the MOK schemes, we do so on the basis of time per matched filter T_{MF}. In the case of DPSK, T_{MF} is twice the time per data symbol or bit. Thus, the time per bit T_b for DPSK is equivalent to that of MOK, M = 4 or $T_{MF}/2$.* Note that for the MOK schemes T_{MF} is equivalent to the time per data symbol T_s. Hence, for MOK we have

$$T_b = T_s/\log_2 M = T_{MF}/\log_2 M. \tag{5.1}$$

Therefore, for MOK

*In other words DPSK is run at twice the bit rate of BOK.

$$T_b/T_{MF} = 1/\log_2 M. \tag{5.2}$$

Similarly, if E_s is the signal energy in time T_{MF}, then the energy per bit is

$$E_b = E_s/2 \text{ for DPSK}, \tag{5.3}$$

$$E_b = E_s/\log_2 M \text{ for MOK}. \tag{5.4}$$

It is desirable to minimize the required E_b/N_o and T_b/T_{MF} for a given message reliability, since signal detectability and message length are important in the IFF context.

With these parameters defined, we want to make a realistic comparison of the various modulation schemes. Suppose we have a message of L bits which must be encoded into symbols and transmitted over the noisy channel. The probability of a message error P_{ME} for MOK in terms of the probability of a symbol error P_{SE} becomes

$$P_{ME} = 1-(1 - P_{SE})^{L/\log_2 M}, \tag{5.5}$$

since $L/\log_2 M$ is the number of symbols required to send L message bits.

For comparison purposes, we will choose L = 60 bits in order that the message can be sent by an integer number of symbols for the MOK, M = 2, 4, 8, 16 and 32 modulation schemes. Also, we will assume a message reliability of 99% or P_{ME} = .01. The corresponding symbol error probabilities for this message length and reliability are given in Table 5.1

Table 5.1

Probability of a symbol error
required for P_{ME} = .01

M	$60/\log_2 M$	P_{SE}(MOK)
2	60	1.675×10^{-4}
4	30	3.350×10^{-4}
8	20	5.024×10^{-4}
16	15	6.698×10^{-4}
32	12	8.372×10^{-4}

The required signal-to-noise ratios per bit E_b/N_o were calculated for the corresponding required symbol error probabilities listed in Table 5.1 and plotted in Fig. 5.1 for the zero doppler case. Notice that we gain both in terms of E_b/N_o and T_b/T_{MF} for the higher order M-ary systems. Of course, we gain at the expense of added complexity of the receiver.

Notice that DPSK gains 3 dB over BOK while operating at twice the bit rate. Also, DPSK is approximately .2 dB better than MOK, M=4 for the same bit rate. It appears advantageous to consider a 16-ary system since the gain from M=8 to M=16 is substantial. A 32-ary system seems less feasible since the added complexity yields less than 1 dB improvement in E_b/N_o and only a 5% decrease in message length over the 16-ary system.

Figure 5.2 compares the same modulation schemes for a fixed doppler shift of $\omega_d T = 1$ radian. The zero doppler points are included to give a relative perspective of the effect of the doppler shift. The MOK schemes are also compared for the ideal case when the phase waveforms are chosen to maintain orthogonality for all doppler shifts. Notice that in this ideal case the relative positions of the MOK schemes remain the same.

DPSK does not perform as well as MOK, M=4 at $\omega_d T = 1$ radian. In fact, MOK, M=4 is approximately .3 dB better than DPSK with the message set defined as the first four Walsh functions and 1.3 dB better than DPSK when the message

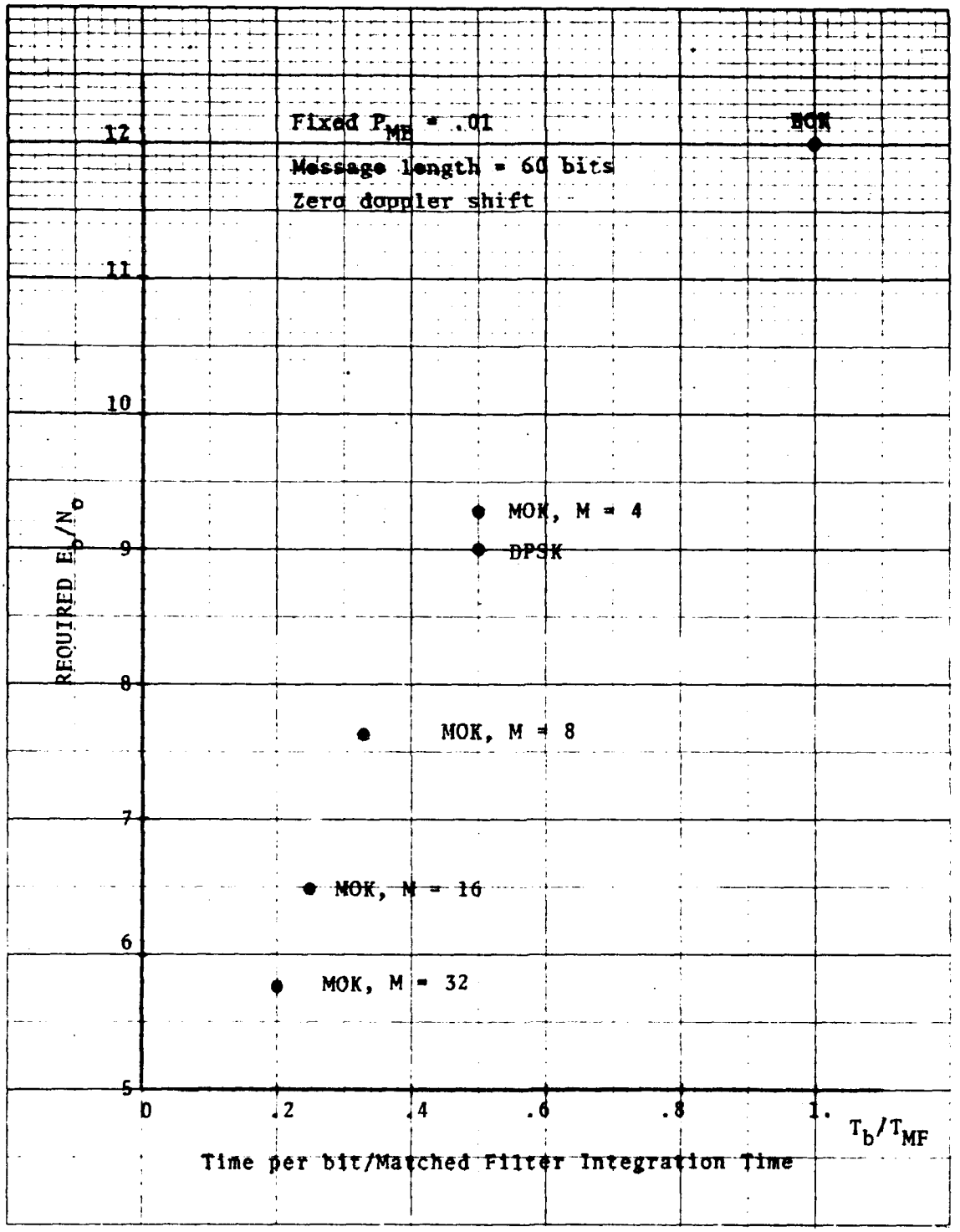

Fig. 5.1. Relative comparison of several modulation schemes for zero doppler shift.

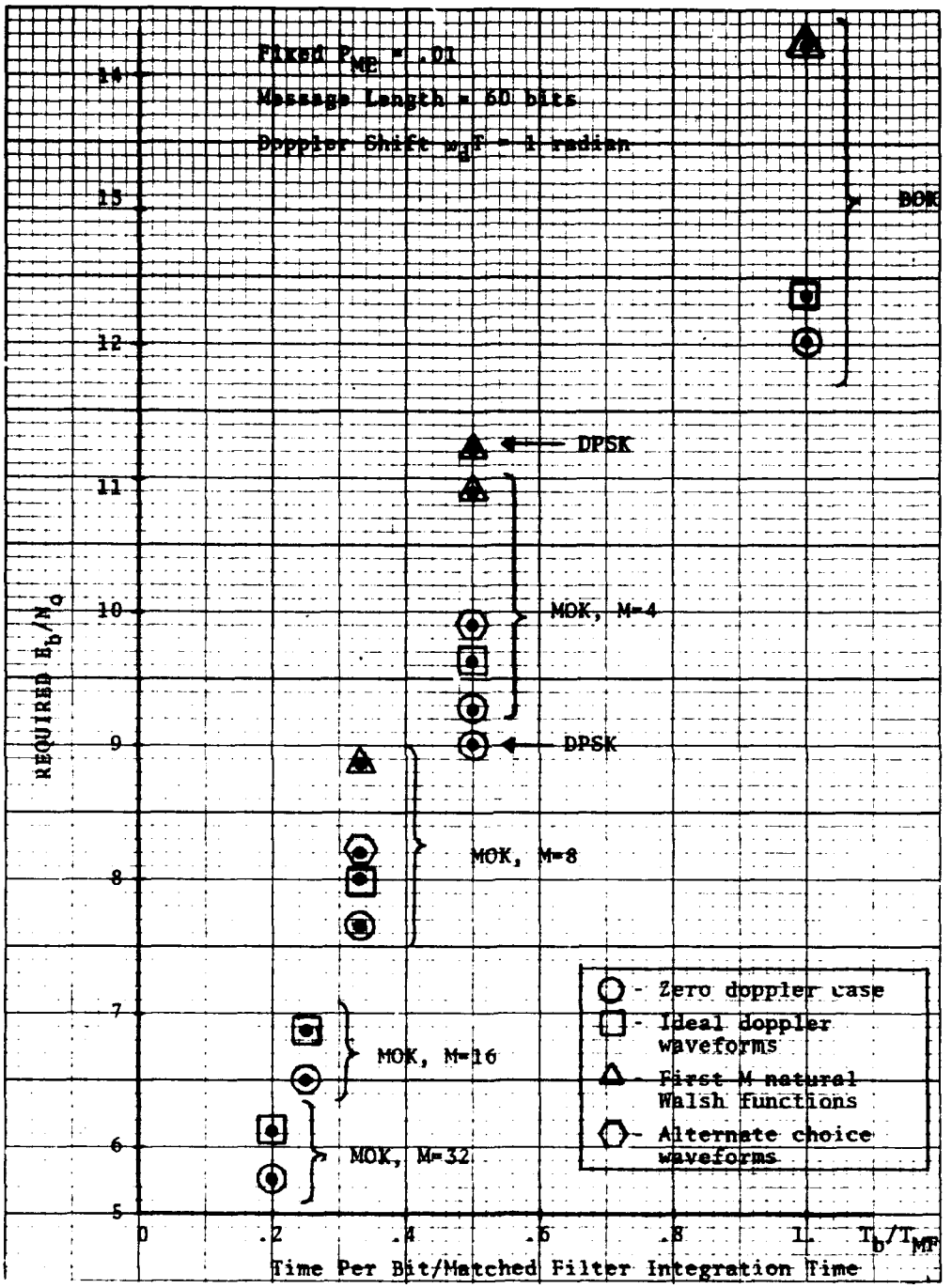

Fig. 5.2. Comparison of several modulation schemes and waveform designs for $\omega_d T$ = 1 radian.

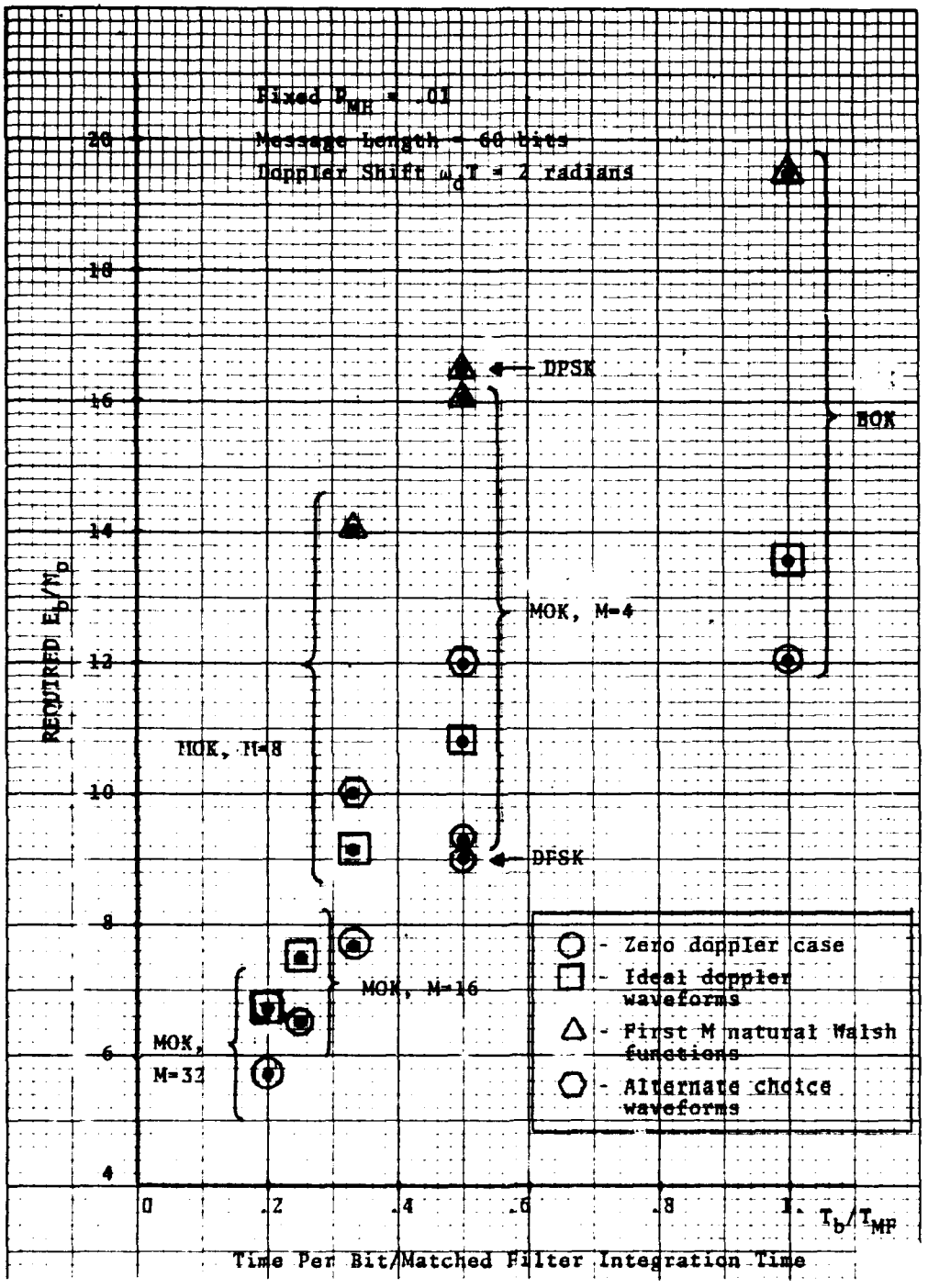

Fig. 5.3. Comparison of several modulation schemes and waveform designs for $\omega_d T = 2$ radians.

set consists of the alternate choise waveforms (WAL(i,t), i=0,3,4 and 7)*. Notice that the altnernate choice waveforms gain approximately .65 dB for the MOK, M=8 case.

Figure 5.3 compares the same modulation schemes for a fixed doppler shift of $\omega_d T = 2$ radians. As expected, there is a substantial increase in the required E_b/N_o for all of the modulation schemes. The most noticeable feature of this plot is the dramatic improvement in E_b/N_o obtained using the alternate choice waveforms in the MOK, M=4 and 8 cases. In both of these cases there is about a 4 dB gain in E_b/N_o.

Significant performance improvements can be obtained by going to a M-ary system for $\log_2 M = 2$, 3, or 4. For $\log_2 M \geq 5$, the increase in performance may not be worth the added receiver complexity. DPSK has close to the same performance as MOK, M=4 when operated at twice the bit rate of BOK.

Proper waveform design yields significant performance improvement in proportion to the value of the doppler shift parameter $\omega_d T$.

*See Fig. 4.3(b).

6.0 CONCLUSIONS

A performance comparison of MDPSK and MOK shows that MOK is much better for $M > 4$ due to the non-orthogonality of the MDPSK signal sets. Furthermore, the degradation of MDPSK, $M = 4$ due to carrier frequency offsets (doppler shift) is greater than the corresponding degradation of MOK, $M = 4$. DPSK (i.e., MDPSK, $M = 2$) has close to the same performance as MOK, $M = 4$ when operated at twice the bit rate of BOK.

Significant performance improvements can be obtained by going to an MOK modulation scheme for values of M greater than four both in terms of the signal-to-noise ratio per information bit E_b/N_o required for a fixed message error performance and in terms of shorter messages. Short messages are important in reducing self interference. For $M \geq 32$, the increase in performance may not be worth the added receiver complexity.

The choice of the orthogonal signal set is important in evaluating the sensitivity of MOK to doppler frequency shift. When a Walsh function signal set is chosen, the ultimate performance obtainable with a carrier frequency offset (due to doppler shift) is limited by the lowest frequency Rademacher function in the set (excluding the identify function, $R_o(t)$).

By using Walsh function signal sets, a single M segment synchronized convolver can be used as a M-ary matched filter. A single PN code is used to spread the signal with one of M Walsh functions providing the additional phase

modulation for M-ary data signalling. In section 4.0 a unique method is shown for implementing an M-ary signal set with a convolver which has $2^n M$ segments (for good doppler performance) with only $1/2M \log_2 M$ sum-difference hybrids.

APPENDIX A

Note the following identities:

$$\sum_{n=1}^{m} (-1)^n \cos n\theta = -\frac{1}{2} + (-1)^m \frac{\cos(m+1/2)\theta}{2\cos\theta/2} \qquad \text{(A-1)}$$

$$\sum_{n=1}^{m} (-1)^n n \cos n\theta = \frac{1}{4(1+\cos\theta)^2} \left\{ -2(1+\cos\theta) + (-1)^m \left[(m+1)\cos(m-1)\theta \right.\right.$$

$$\left.\left. + (3m+2)\cos m\theta + (3m+1)\cos(m+1)\theta + m\cos(m+2)\theta \right] \right\} . \qquad \text{(A-2)}$$

The output of tne envelope detector from (2) is

$$y_o(t_s) = \sqrt{E} \left| \operatorname{sinc} \frac{\omega_c T}{2N} \right| \sqrt{\frac{1}{N} + \frac{2}{N^2} \sum_{i=1}^{N-1} (N-i)(-1)^i \cos i \frac{\omega_c T}{N}} . \qquad \text{(A-3)}$$

For large values of N the identities (A-1) and (A-2) can be used to yield

$$|y_o(t_s)|^2 \cong \begin{cases} E/N^2 \sin^2 \omega_c T/2 & N \text{ even} \\ E/N^2 \cos^2 \omega_c T/2 & N \text{ odd} \end{cases} . \qquad \text{(A-4)}$$

Thus, regardless of the doppler frequency shift, the output squared (or effective energy) of the not true matched filter goes to zero as $1/N^2$ as $N \to \infty$. Note that the approximation given by (A-4) is very good for $N \geq 8$.

REFERENCES

1. W. C. Lindsey and M. K. Simon, Telecommunication Systems Engineering, (Prentice-Hall, 1973).

2. J. T. Fleck, and E. A. Trabka, "Error Probabilities of Multiple-State Differentially Coherent PSK Systems in the Presence of WGN," Report No. VA-1420-S-1, Cornell Aeronautical Laboratory, Inc., Buffalo, NY, 1961.

3. E. Arthurs and H. Dym, "On the Optimum Detection of Digital Signals in the Presence of WGN," IEEE Trans. Commun., CS-10, No. 4., (1962).

4. J. J. Bussgang and M. Leiter, "Error Rate Approximations for DPSK," IEEE Trans. Commun., CS-12, No. 1, (1964).

5. J. H. Cafarella, Private Communication.

6. K. G. Beauchamp, Walsh Functions and Their Applications, (Academic Press, London, 1975).

REPORT DOCUMENTATION PAGE

Form Approved
OMB No. 0704-0188

1. AGENCY USE ONLY (*Leave blank*)	2. REPORT DATE	3. REPORT TYPE AND DATES COVERED
	29 September 1981	Project Report

4. TITLE AND SUBTITLE

Data Modulation for a Direct Sequence Pseudonoise Spread Spectrum Communication System

5. FUNDING NUMBERS

C — F19628-80-C-0002
PR — 309

6. AUTHOR(S)

Alan L. Kachelmyer

7. PERFORMING ORGANIZATION NAME(S) AND ADDRESS(ES)

Lincoln Laboratory, MIT
P.O. Box 73
Lexington, MA 02173-9108

8. PERFORMING ORGANIZATION REPORT NUMBER

IFF-7

9. SPONSORING/MONITORING AGENCY NAME(S) AND ADDRESS(ES)

Aeronautical Systems Division
Wright Patterson AFB, Ohio 45433

10. SPONSORING/MONITORING AGENCY REPORT NUMBER

ESD-TR-90-194

11. SUPPLEMENTARY NOTES

None

12a. DISTRIBUTION/AVAILABILITY STATEMENT

Approved for public release; distribution is unlimited.

12b. DISTRIBUTION CODE

13. ABSTRACT (*Maximum 200 words*)

This report considers the incoherent demodulation performance of M-ary orthogonal keying (MOK) and M-ary differential phase shift keying (MDPSK) in the presence of a Doppler frequency shift of the carrier. It is shown that MOK has a significant performance improvement over MDPSK for values of M greater than four in terms of the required signal-to-noise ratio per information bit. The choice of the orthogonal signaling set is important in evaluating the sensitivity of MOK to Doppler frequency shift. If Walsh function signaling sets are to be chosen, then the ultimate performance in Doppler is limited by the lowest frequency Rademacher function in the signaling set. A single M segment can be used to implement the M-ary matched filter. By increasing the number of convolver segments, signaling sets with better performance in the presence of a Doppler frequency shift can be implemented.

14. SUBJECT TERMS		15. NUMBER OF PAGES
M-ary orthogonal keying (MOK) M-ary differential phase shift keying (MDPSK) Doppler frequency shift	matched filter Walsh functions Rademacher functions acousto-electric convolver	80 16. PRICE CODE

17. SECURITY CLASSIFICATION OF REPORT	18. SECURITY CLASSIFICATION OF THIS PAGE	19. SECURITY CLASSIFICATION OF ABSTRACT	20. LIMITATION OF ABSTRACT
Unclassified	Unclassified	Unclassified	SAR